Naval Research Laboratory

Stennis Space Center, MS 39529-5004

NRL/MR/7330--15-9547

Validation Test Report for the Automated Optical Processing System (AOPS) Version 4.10

Sherwin Ladner
Richard Crout
Adam Lawson

Ocean Sciences Branch
Oceanography Division

Paul Martinolich
Jennifer Bowers

Vencore Incorporated
Chantilly, Virginia

Giulietta Fargion

San Diego State University
San Diego, California

Robert Arnone
Ryan Vandermeulen

University of Southern Mississippi
Hattiesburg, Mississippi

August 25, 2015

REPORT DOCUMENTATION PAGE

Form Approved
OMB No. 0704-0188

1. REPORT DATE *(DD-MM-YYYY)*
25-08-2015

2. REPORT TYPE
Memorandum Report

3. DATES COVERED *(From - To)*

4. TITLE AND SUBTITLE

Validation Test Report for the Automated Optical Processing System (AOPS) Version 4.10

5a. CONTRACT NUMBER

5b. GRANT NUMBER

5c. PROGRAM ELEMENT NUMBER
0601153N

6. AUTHOR(S)

Sherwin Ladner, Richard Crout, Adam Lawson, Paul Martinolich,[a] Jennifer Bowers,[a] Giulietta Fargion,[b] Robert Arnone,[c] and Ryan Vandermeulen[c]

5d. PROJECT NUMBER

5e. TASK NUMBER

5f. WORK UNIT NUMBER
73-4948-04-5

7. PERFORMING ORGANIZATION NAME(S) AND ADDRESS(ES)

Naval Research Laboratory
Oceanography Division
Stennis Space Center, MS 39529-5004

8. PERFORMING ORGANIZATION REPORT NUMBER

NRL/MR/7330--15-9547

9. SPONSORING / MONITORING AGENCY NAME(S) AND ADDRESS(ES)

Office of Naval Research
One Liberty Center
875 North Randolph Street, Suite 1425
Arlington, VA 22203-1995

10. SPONSOR / MONITOR'S ACRONYM(S)

ONR

11. SPONSOR / MONITOR'S REPORT NUMBER(S)

12. DISTRIBUTION / AVAILABILITY STATEMENT

Approved for public release; distribution is unlimited.

13. SUPPLEMENTARY NOTES

[a]Vencore Inc., 15052 Conference Center Dr., Chantilly, VA
[b]San Diego State University, 5500 Campanile Dr., San Diego, CA 92182
[c]University of Southern Mississippi, 118 College Drive, Hattiesburg, MS 39406

14. ABSTRACT

This document describes the testing and evaluation of the Automated Optical Processing System (AOPS) version 4.10 for the Moderate Resolution Imaging Spectrometers (MODIS-Aqua), Visible Infrared Imager Radiometer Suite (VIIRS), and the Geostationary Ocean Color Imager (GOCI) sensors. AOPS enables exploitation of multiple space-borne ocean color satellite sensors to provide optical conditions for operational Navy products supporting Mine Warfare (MIW), Naval Special Warfare (NSW), Expeditionary Warfare (EXW), and Anti-Submarine Warfare (ASW). Ocean optical products are used to predict the impact of the environment on diver operations, communications, mine detection, and target detection. As part of this evaluation, inter-sensor satellite-derived ocean color properties (nLw,IOPs) comparisons are made. In addition, all sensors-derived ocean color properties are evaluated against in situ data from ocean cruises and comparison with the Aerosol Robotic Network-Ocean Color (AERONET-OC) SeaPrism sensors. These comparisons show that MODIS, VIIRS, and GOCI generate high quality ocean color products and should provide a continued data stream to support operational products.

15. SUBJECT TERMS

Satellite	MODIS	Matchups	Inherent Optical Properties
Ocean color	VIIRS	Calibration	IOP
Remote sensing	GOCI	Validation	Operational

16. SECURITY CLASSIFICATION OF:			**17. LIMITATION OF ABSTRACT**	**18. NUMBER OF PAGES**	**19a. NAME OF RESPONSIBLE PERSON**
a. REPORT	**b. ABSTRACT**	**c. THIS PAGE**			Sherwin Ladner
Unclassified Unlimited	Unclassified Unlimited	Unclassified Unlimited	Unclassified Unlimited	45	**19b. TELEPHONE NUMBER** *(include area code)* 228-688-5754

Standard Form 298 (Rev. 8-98)
Prescribed by ANSI Std. Z39.18

Validation Test Report for the Automated Optical Processing System (AOPS) Version 4.10

Contents

1 Introduction

Work performed under the Space and Naval Warfare Systems Center (SPAWARSYSCEN) Preparing Tactical Ocean Optical Products from Future Polar-Orbiting Sensors project enables exploitation of the Visible Infrared Imager Radiometer Suite (VIIRS) and similar ocean color sensors to provide Navy products for operational use. Work completed was in response to the Navy's need to exploit all available remote sensing technologies[1] as part of a larger effort to provide a continuous operational picture of environmental conditions of the battlespace.

This Validation Test Report (VTR) provides the technical bases to transition the Automated Optical Processing System (AOPS) version 4.10 to the NP3 Ocean Optics branch of the Naval Oceanographic Office (NAVOCEANO). AOPS is the software that allows NAVOCEANO to describe operational ocean optical conditions from satellite imagery. AOPS is used by NAVOCEANO to support fleet operators engaged in Naval Special Warfare (NSW), Mine Warfare (MIW), Expeditionary Warfare (EXW), and Anti-Submarine Warfare (ASW). Additionally, these same products are used in real time to support analysis of ocean models by oceanographers on the NAVOCEANO watch floor.

The project was divided into four task areas, where AOPS is identified as the transitioning element of the project. As the transition, AOPS v4.10 provides tools and algorithms to process data from environmental remote sensing satellites in accordance with the Meteorology and Oceanography (METOC) Space Satellite readiness plan and enables rapid dissemination of final products via NAVOCEANO's web portal and other avenues compliant with distribution policies. The AOPS collection of programs allows scientists to generate co-registered image databases of geophysical parameters derived from remotely sensed data. To accomplish this, AOPS uses the techniques of *extension* and *automation*.

Extension is the use of small programs, each designed for a specific task, and a shell to 'glue' them together. The idea is similar to the UNIX operating system and its many programs like **cat**, **tr**, **basename**, etc. and allows the user to augment the system with their own features and programs.

Automation is the technique of operating a system without human effort or decision. For AOPS, this is achieved by setting up a directory structure and using scripts to monitor the directories for new input data -- as new data is made available to the system, it is processed without user intervention.

---

[1] In light of the aging MODIS satellites and current status of the DWSS program, the Joint Polar Satellite System (JPSS) satellite and other foreign sensors are expected to be the primary sources of DOD METOC data for the next 20 years. Naval operations will rely on the integration of these sensors into current operational processing to provide continuity of legacy products and spatial coverage of current operational areas.

Manuscript approved October 16, 2014.

AOPS does not contain GUIs or visualization programs; therefore all user input *must* be provided to the program upon *start*.

2 System Description

AOPS is a collection of UNIX programs and shell scripts that enables automated generation of map-projected image data bases of satellite derived products from streaming raw satellite data. Individual scenes are sequentially processed from the raw digital counts (Level-1) using standard parameters to a radiometrically and geometrically corrected (Level-3) product within several minutes. AOPS further processes the data into a variety of temporal composites called mosaics (Level-4). These products are stored in the Hierarchical Data Format (HDF) with specific attributes. Additionally, it automatically generates quick-look "browse" images in JPEG format.

AOPS uses a simple monitoring technique. The main driver regularly polls a specified input directory for incoming data and for each file found, executes what are known as `areas` scripts on the file in a working directory. The `areas` scripts do the actual construction of the desired results (i.e. the data bases). After each areas script has been run on the file, it is moved to an output directory. This method uses the directory as the queuing system for data to be processed.

The 4.10 version represents the most recent processing algorithms employed at the Naval Research laboratory as of 10 Dec 2013, for current operational sensors. The system has been developed on CenTOS 5.7 (x86, x86_64) – equivalent to RHEL v5.

Historically, AOPS was capable of processing data from: Sea-viewing Wide Field-of-view Sensor (SeaWiFS), Moderate Resolution Imaging Spectrometers (MODIS on Aqua), and Medium Resolution Imaging Spectrometer (MERIS)[2]. This VTR documents the new capability in AOPS to produce operational products from the Joint Polar Orbiting System (JPSS) – Suomi National Polar-orbiting Partnership (NPP) with the VIIRS sensor package as well as from the Geostationary Ocean Color Imager (GOCI) sensor aboard the Communication Ocean and Meteorological Satellite (COMS) satellite. It also includes algorithm improvements requested by NAVOCEANO. Additional upgrades in AOPS v 4.10 provide improved operational products from the MODIS sensor due to calibration updates.

Sensor characterization is critical in order to use the end products for navy support because the ocean color signal represents only ten percent of the total radiance signal at the top of the atmosphere (TOA). Errors in sensor calibration, out of spectral band response issues, polarization and atmospheric correction must be accounted for so that operational products can be accurate and provide consistency with existing ocean color products[3].

---

[2] MERIS and SeaWiFS have been removed as both satellites have stopped working.

[3] Navy products from AOPS include: diver visibility, laser penetration depth, chlorophyll concentration, and inherent optical products[3]. In addition to providing a depiction of the environment, the products can be used for validation of or assimilation

The VTR for AOPS v4.10 describes the testing and data comparisons necessary to demonstrate that the products derived from the VIIRS sensor can be used for navy operations and should be integrated into NAVOCEANO operations to support the fleet.

We will demonstrate the operational capability of AOPS by showing:

- VIIRS matchups with *in situ* data collection sites such as The Marine Optical BuoY (MOBY) and the AErosol RObotic NETwork – Ocean Color (AERONET-OC) sites
- Comparison of MODIS and VIIRS products such as diver visibility and inherent optical properties (IOPs).
- Performance of GOCI sensor compared to AERONET-OC, VIIRS and MODIS where available.

2.1 System Requirements

AOPS runs in the Red Hat Enterprise Linux (RHEL) environment. Users should be familiar with UNIX; BASH shell programming; and remote sensing, particularly regarding computer processing of satellite data. The system memory and storage requirements are difficult to gauge. The amount of memory needed is dependent upon the amount and type of satellite data you wish to process; the larger the area, the larger the memory requirement. For example, the entire Atlantic Ocean will require more processing power than the Mississippi Bight. In addition, the type of data being processed will determine how robust the system should be. Data storage requirements are a function of the temporal and spatial needs of both the NAVOCEANO system operators and the data consumers. A technical description for how to use AOPS that would enable identification of memory and disk space requirements is provided in the AOPS Users Guide v 4.10, 2013.

2.1.1 Data Input

Currently AOPS supports VIIRS inputs provided by the Air Force Weather Agency (AFWA) stream delivered to NAVOCEANO. A redundant data stream is available through NOAA's Comprehensive Large Array-data Stewardship System (CLASS) and Government Resource for Algorithm Verification, Independent Testing and Evaluation (GRAVITE) systems. At the time of this writing the three data sources are identical therefore after establishing data subscriptions, processing is transparent.

The GOCI inputs are provided to NAVOCEANO from the Korea Ocean Research and Development Institute (KORDI). A redundant data stream has been proposed through the Ocean Biology Processing Group (OBPG) though as of the writing the system is not operational.

---

into ocean forecast models. Ocean optical products are used to predict the impact of the environment on navy systems used in communication, mine detection and target detection.

2.1.2 AOPS Output

The AOPS format is based on the Scientific Data Sets interface in version 4 of the Hierarchical Data Format (HDF4). No other interface or objects are used or allowed in a valid APS file.

Within the Scientific Data Sets subset, a valid APS file is limited to an array of no more than three dimensions one of which may be UNLIMITED. All standard number types (INT8, UINT8, INT16, UINT16, INT32, UINT32, FLOAT32, FLOAT64, and CHAR8) may be used.

None of the pre-defined attributes using such API's as SDgetdatastrs(), for example, are used. The APS format supports both file and data set attributes. The APS format has several required file and data set attributes that must exist with each file or data set, respectively.

There is no limit to the number of data sets other than those imposed by the HDF4 library. However, there are some limits placed on the names of general data set names.

The APS IO library contains routines for accessing all objects from the APS file. Use of this library is strongly encouraged as the underlying file structure may change. The AOPS User's Guide v4.8, 2012 describes the file format structure as well as the use of the library.

2.1.2.1 Level 3 Regional Data Products

AOPS generates radiometrically and geometrically corrected (Level-3) products within several minutes. There are a *variable* number of data sets in an AOPS Level-3 Regional Data Product file. The *meta data sets* are standard, providing geographical coverage and data quality information. The p*roduct data sets* contain the actual geophysical products and vary in number. A long descriptive name is used to facilitate use of the p*roduct data sets*, and in some cases, the algorithm used is also provided in the name. Examples are "Remote Sensing Reflectance at 443 nm" and "Chlorophyll Concentration, OC4 Algorithm". File attributes are associated with all products in the HDF file. The attributes are divided into several groups and a detailed discussion can be found in the AOPS Users Guide, 2013.

2.1.2.2 Level-4 Regional Data Products

AOPS also generates several different temporal composites (Level-4). The Level-4 Regional Data Product File contains atmospherically corrected geophysical products in a standard map projection for a specific region of interest derived from one of several different satellites (GOCI, MODIS, and VIIRS). A Level-4 Regional Data Product may be stored in one of several formats. The default is stored using HDF developed by the National Center for Supercomputer Applications (NCSA) at U. of Illinois Urbana-Champaign (version 4.2.8). Additional output file types that are supported include: version 5 of the HDF format (using HDF5 v1.8.6) and the netCDF v4. A technical description can be found in the AOPS Users Guide, 2013.

3 Validation Test descriptions

Traditional *ground truthing* with *in situ* observations is one of two approaches to evaluate the VIIRS ocean color products. VIIRS products are compared to *in situ* data collected at the MOBY site, AERONET-OC network, and oceanographic cruise data collection. The second approach for evaluating NPP ocean color products is direct comparison with existing satellite products such as MODIS. This cross-platform approach will enable consistent data sets from which global metrics of the NPP products can be established. Furthermore, cross-platform calibration will allow validation of products in critical coastal regions where *in situ* data is not available.

Calibration and Validation Process

In situ bio-optical global and coastal measurements have a critical function in satellite calibration/validation (cal/val) activities, the development of remote-sensing algorithms and statistical models that convert radiometric measurements (water leaving radiance or surface reflectance) to geophysical data products (chlorophyll a and others). The quality of these cal/val and conversion algorithms cannot be better than that of the data sets of ocean properties used to create them.

In situ data collected for cal/val uses the same measurements and the same methodologies, but calibration requires lower measurement uncertainties. This means that the sampling site must have minimal natural variability (oceanic and atmospheric), in order to reduce the total uncertainty (Hooker et al., 2007). Today, the ocean color community views *in situ* data as having variable quality, and therefore these data should be ranked by quality for different purposes (from highest quality to lowest): calibration, validation/algorithm development, general research and monitoring. Guidelines for calibration/validation (cal/val) field programs are:

1. Data collected in a stable environment (spatially & temporally homogeneous; and known atmospheric conditions) and sufficiently far from land (>5km);
2. Sample all measurements necessary to produce good water leaving radiance data. Measurements should have well defined uncertainties quantified, collected with appropriate methodologies (approved protocols), with calibrated instruments (pre/post-cruise calibrations that are traceable). Cal/val team should define set of parameters to be measured to have cross-site consistency;
3. Sample as close to satellite overpass as possible, preferably in a time-series. Continuous data will have higher match-up retrievals and will allow for assessment of products for successive missions;
4. Globally distributed *in situ* data to fully represent the wide range of geophysical conditions that remote sensing is expected to observe; and
5. Consistent data processing with a clear QA/QC process.

MOBY[4] and BOUée pour l'acquiSition d'une Série Optique à Long termE (BUSSOLE) buoys are the primary cal/val sites and both comply with the above calibration guidelines. These buoys have been the primary basis for the on-orbit vicarious calibrations of the USA Sea-viewing Wide Field-of-view Sensor (SeaWiFS), the Japanese Ocean Color and Temperature Sensor (OCTS) and Global Imager (GLI), the

French Polarization Detection Environmental Radiometer (POLDER), the USA Moderate Resolution Imaging Spectrometers (MODIS, Terra and Aqua), the Japanese Global Imager (GLI), and the European Medium Resolution Imaging Spectrometer (MERIS).

Because the MODIS sensor is aging, the satellite oceanography community is working to have the VIIRS mission be operational as soon as possible. With this goal, a revised methodology was developed to do near real time cal/val activities. This requires modification to data guidelines (mainly point 1) and changes to exclusion criteria currently used by the NASA Ocean Biology Processing Group (OBPG). The stability and scan characteristics of the VIIRS sensor at an early stage in the mission, requires the use of coastal and open ocean validation and calibration sites. Real time coastal sites, though of lower quality, have been successfully used to monitor sensor stability and provide sufficient "matchups" in real time to perform more routine updates of the vicarious calibration.

The current procedure for ocean color cal/val following the OBPG approach (Figure 1) requires several years of coincident satellite and high quality *in situ* data before applying calibration gains and sufficient matchups to produce algorithm validation[4] (Bailey and Werdell, 2006). By allowing flexibility of the screening process and utilizing the daily coastal AERONET-OC real–time sites, statistically significant matchups are generated. These data have some QA/QC, initial calibration, sampling and processing protocols, but also have higher ocean/atmospheric variability. Further, we have successfully used these AERONET sites for coastal calibration (satellite gains) and algorithm improvement.

The vicarious adjustment calculations (calibration) are performed using *in situ* spectral radiance propagated to Top of Atmosphere (TOAv) for each satellite to form a ratio ("gain") with the spectral TOAs of the satellite using the standard atmospheric correction of Gordon/Wang (1994) with a NIR iteration (Stumpf, et. al) assuming perfect sensor calibration in the NIR channels. These gain adjustments have been computed for MOBY (open ocean) and for each AERONET (coastal ocean) to calibrate and track the product performance for VIIRS. The process begins by performing the initial atmospheric correction of the input VIIRS Lt to obtain the nLw at the point in question. The various atmospheric components (Lr, La, transmittances, etc.) and pointing-angles are saved during this process. nLw is then replaced with the in-situ (convolved MOBY or hyper spectral model shifted AERONET) derived values. The atmospheric components are added to the replaced nLw to obtain a new Lt from the view of the VIIRS. This new Lt is known as the vicarious Lt (vLt). In a perfect system in which all components are computed accurately, the vLt and original Lt should have a ratio of 1.0.

[4] Over 9-years, MOBY provided about 1450 contemporaneous match ups for SeaWiFS and only 150 match-ups passed the stringent screening processes for long-term vicarious calibration (*approximately 17 per year*). BOUSSOLE Project information is available at http://www.obs-vlfr.fr/Boussole/

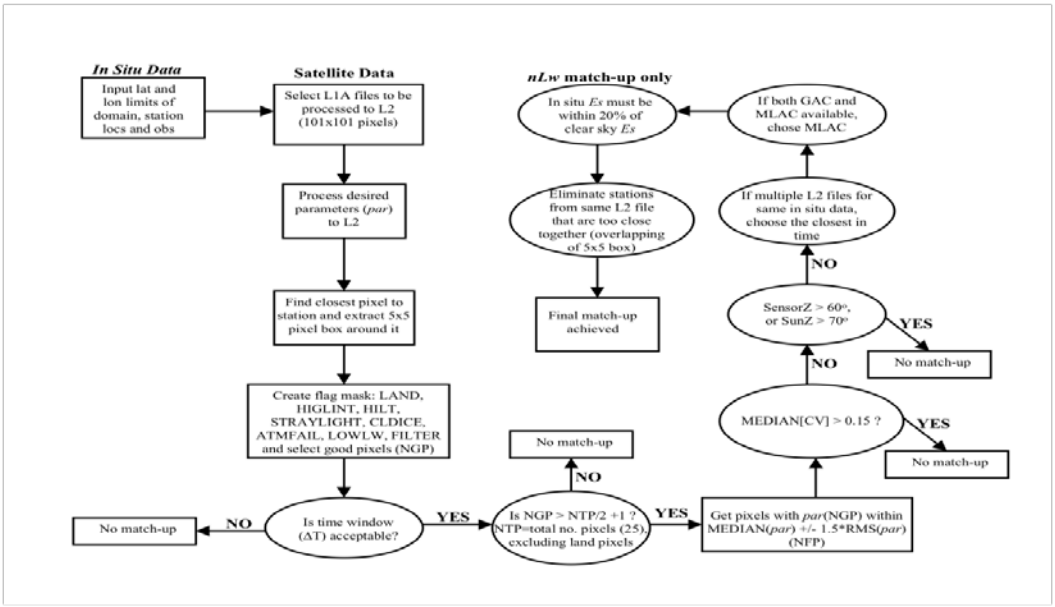

Figure 1 Match-up procedure for comparing *in situ* and satellite data employed by NRL is similar to that used by NASA OBPG.

The Satellite Validation Navy Tool (SAVANT) provides NRL the semi-automated capability for preforming flexible validation match-up analysis following the NASA OBPG procedures. For validation match-ups, we use the AERONET sites (nLw, Level 1.5) and the satellite (Level 3). The satellite spatial box can be set to a single pixel, or 9km^2 or 25km^2 centered on the *in situ* data (lat, long). Exclusion criteria which can be set in SAVANT are:

- The time window can be set to define coincident as ± 1hr to ± 3 hours, in 30 minute increments.
- *In situ* data are typically screened as follows:
  - exclude wind speeds > 8 m/s
  - set a maximum Aerosol Optical Thickness (AOT) = 0.2
  - set the minimum nLw value = 0
  - set the maximum nLw value = 3
- Satellite data can be screened as follows:
  - set the maximum Coefficient of Variance = 0.30
  - set the minimum percent valid pixel requirement to 50
  - set the satellite box size = single pixel, 9 km (3 km x3km AOI) or 25km (5 km x5 km AOI)
  - set the satellite zenith angle minimum = 0 and maximum = 56
  - set the solar zenith angle minimum = 0 and maximum = 70
  - set the satellite azimuthal angle minimum = -180 and maximum = 180
  - set the solar azimuthal angle minimum = -180 and maximum = 180

- The Level 2 quality flags that can be applied to satellite data allows exclusion of scenes affected by : atmospheric failure, high LT (saturation), could/ice, low water-leaving radiance, land, high satellite zenith angle, high solar zenith angle, navigation failure, high glint, stray light, maximum NIR iteration reached, high polarization, and moderate sun glint.

For this analysis, minimal screening criteria were applied to mimic a more operational testing scenario. Data were limited to within 3 hours with typical *in situ* screening. The satellite was selected as a single pixel unless specifically noted otherwise. The standard exclusionary angles were used, removing viewing angles above 56 degrees and 70 degrees for the satellite and solar zenith angles, respectively. Level 2 quality flags were used to remove records affected by atmospheric failure, navigation failure, clouds/ice, land, high LT, high glint, low water leaving radiance, and max aerosol iteration failure. After accounting for exclusion criteria and processing techniques, the *in situ* data was directly compared to the satellite data to validate the coastal algorithm and track satellite performance over time. The data extracted to support this analysis comes from 1 Jan 2013 to 31 Oct 2013.

The technical details of development and implementation are also provided in the Space and Naval Warfare Systems Command (SPAWAR) FY2013 and FY2014 Monthly Progress Reports, and the originating vicarious calibration papers written by Bailey et al, 2008, and Franz et al 2007.

3.1 *In situ* comparisons

3.1.1 MOBY site gain monitoring

MOBY is a NOAA-funded project that provides data for vicarious calibration of ocean color satellites (Clark, et al 2003). MOBY is located in the waters off Lanai, Hawaii, in 1200 m of water. Since late 1996, it has provided the primary basis for the on-orbit vicarious calibration for the United States, European, and Japanese satellites. The data from this site supports vicarious calibration of individual sensors and supports the international effort to develop a global, multi-year time series of consistently calibrated ocean color data products. MOBY data is currently available in real time, with current uncertainty estimates of approximately 5% for MODIS channels 8 through 12 and 12.5% for channel 13, *due to a large shadowing correction* (Brown et al, 2007).

Figure 2 shows the vLt/Lt over time using unity gains. In a perfect system in which all components are computed accurately, the original Lt and vicarious Lt should have a ratio of 1.0. Most of the ratios are below the 1.0 line suggesting the sensor without vicarious calibration is slightly high. The mean gain for the 412, 442, 490, 555, and 668 channels are 0.9709, 0.9801, 0.9860, 0.9843, and 0.9783 respectively. For comparison, we also processed the data using the vicarious calibration coefficients determined from Feb 2012 to March 2013. Figure 3 shows the vLt/Lt relationship over time by processing the MOBY imagery with the vicarious calibration coefficients. The ratios vary around the 1.0 line suggesting the sensor with vicarious calibration is on average performing better than it does with unity gains. The mean gain for the 412, 442, 490, 555, and 668 channels are 0.9910, 0.9946, 1.0008, 1.0047, and 0.992 respectively. The improvement provided by applying with vicarious calibration is evident as the individual and average gains shown in Figure 3 are closer to the 1.0 ratio.

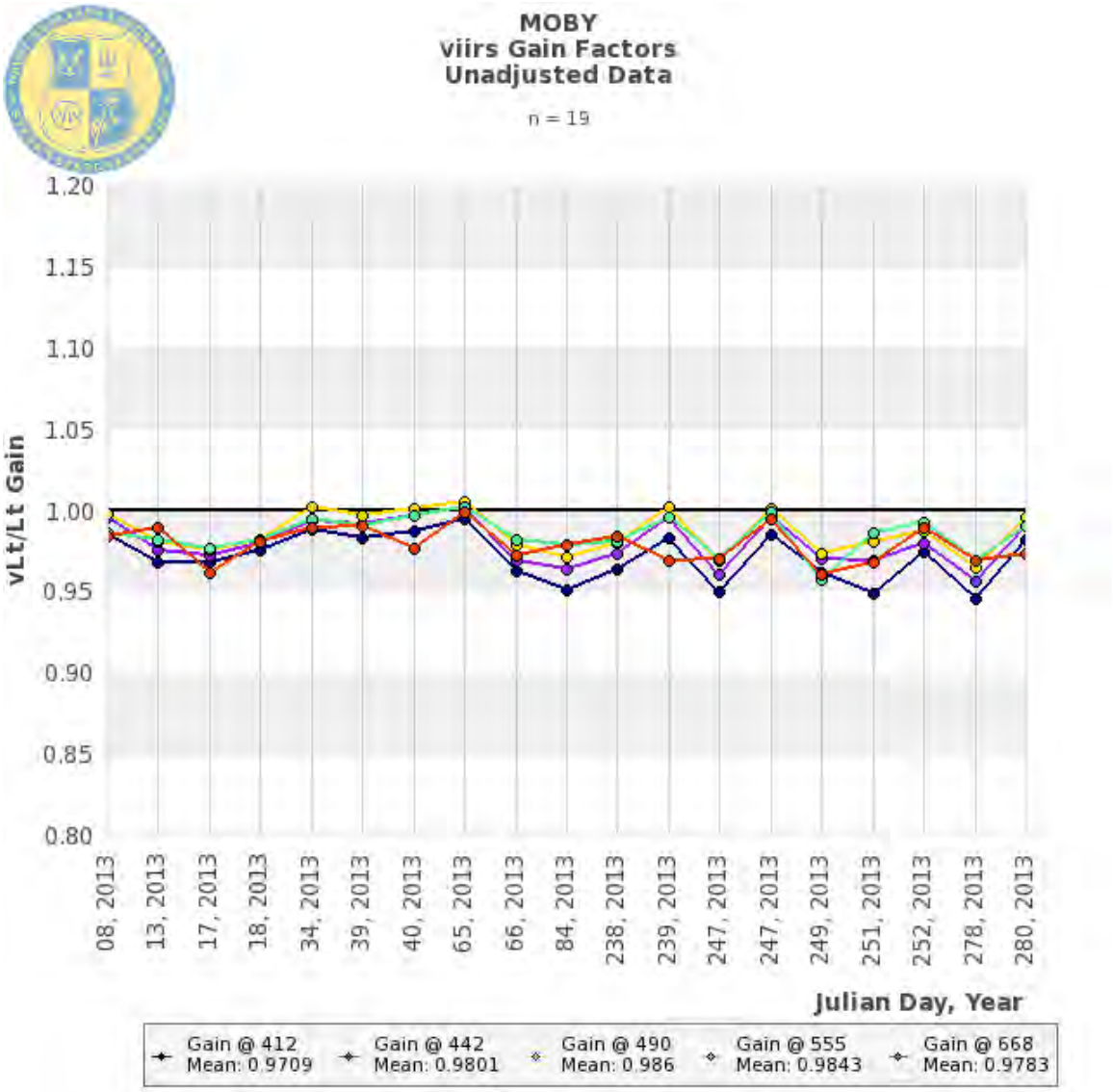

Figure 2 shows the vLt/Lt over time using unity gains. In a perfect system in which all components are computed accurately, the original Lt and vicarious Lt should have a ratio of 1.0. Most of the ratios are below the 1.0 line suggesting the sensor without vicarious calibration is slightly high. The mean gain for the 412, 442, 490, 555, and 668 channels are 0.9709, 0.9801, 0.9860, 0.9843, and 0.9783 respectively.

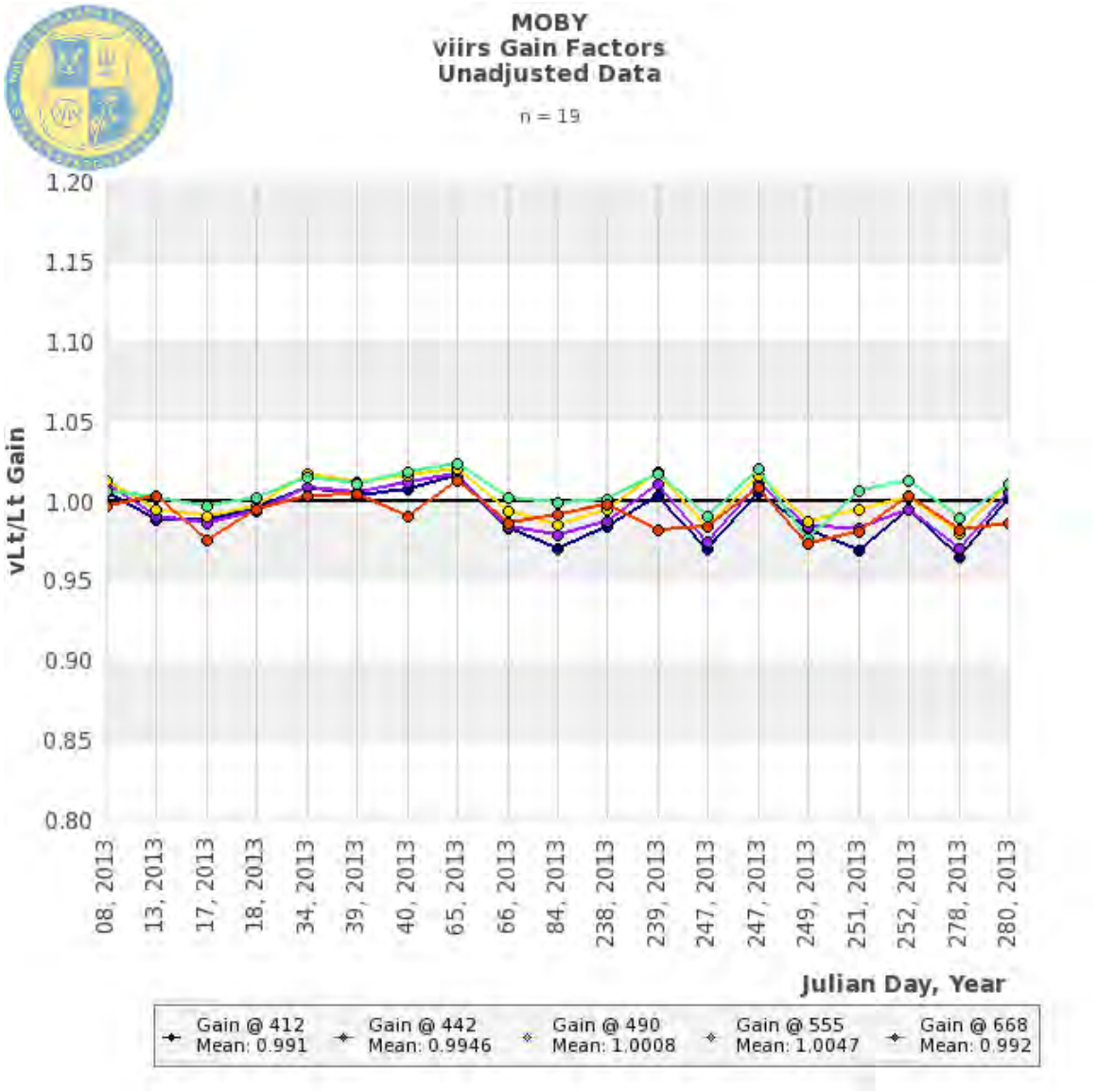

Figure 3 shows the vLt/Lt relationship over time by processing the MOBY imagery with the vicarious calibration coefficients. The ratios vary around the 1.0 line suggesting the sensor with vicarious calibration is on average performing better than it does with unity gains. The mean gain for the 412, 442, 490, 555, and 668 channels are 0.9910, 0.9946, 1.0008, 1.0047, and 0.992 respectively.

3.1.2 AERONET– Analysis

AERONET-OC

AERONET-OC is a sub-network of the Aerosol Robotic Network (AERONET), using modified sun-photometers to support ocean color validation activities with standardized measurements of normalized water leaving radiance and of aerosol optical properties. Autonomous radiometers are operated on fixed platforms in coastal regions. The rational for the AERONET-OC is to assess the accuracies of coastal nLw from current ocean color sensors. Strict criteria exist for data collection, protocols and processing to calculate the nLw for use in satellite product calibration and validation (Zibordi et al. 2009). To use

the AERONET-OC data for near real time cal/val efforts, the NRL process utilizes an intermediate product known as Level 1.5 data. An estimate of the overall uncertainty budget in AERONET-OC Lwn (Level 2) has shown values typically below 5% at the blue and green center wavelengths. Uncertainties around 8% have been estimated for the red center wavelengths (D'Alimonte and Zibordi, 2006; D'Alimonte et al. 2008; Zibordi et al. 2009).

Figure 4 shows the 410 nm nLw matchups for the Venice AERONET site (AAOT/Venise) from 1 Jan 2013 up to 31 Oct 2013. Matchups are between the AERONET-OC location to the single pixel from VIIRS. Matchups are minimally screened, removing: negative values at any wavelength, extreme viewing angles, clouds, navigation failures, atmospheric failures. A red 1:1 line is provided for reference. The regression indicates a *tight* correlation as the VIIRS nLw is 94% of the in situ value. While the correlation coefficient of the 410 nm relationship indicates 79% of the variation in VIIRS is explained by the variation in the AERONET-OC measurement. This r2 is the lowest for the 2013 Venice matchups, however this is expected due to the complex atmospheres and natural variability in water constituents present in coastal waters Figure 5 through Figure 8 show the remaining spectral matchups for the AAOT/Venise site for calendar year 2013.

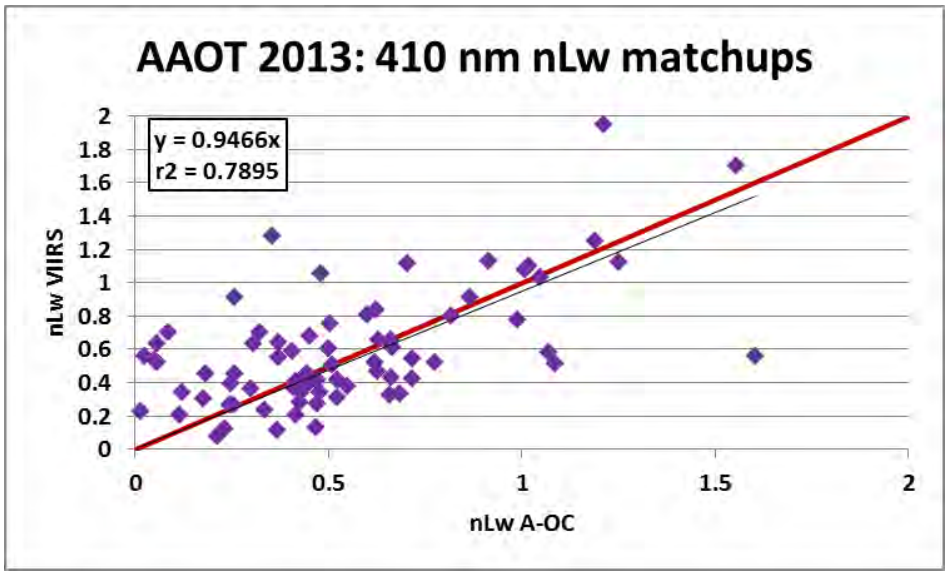

Figure 4 shows the 410 nm nLw matchups for the Venice AERONET site (AAOT/Venise) from 1 Jan 2013 up to 31 Oct 2013. Matchups are between the AERONET-OC location to the single pixel from VIIRS. Matchups are minimally screened, removing: negative values at any wavelength, extreme viewing angles, clouds, navigation failures, atmospheric failures. A red 1:1 line is provided for reference. The regression indicates a tight correlation as the VIIRS nLw is 94% of the *in situ* value. While the correlation coefficient of the 410 nm relationship indicates 79% of the variation in VIIRS is explained by the variation in the AERONET-OC measurement. This r^2 is the lowest for the 2013 Venice matchups, however this is expected due to the complex atmospheres and natural variability in water constituents present in coastal waters, including the complexities of pixel to point matchup variations.

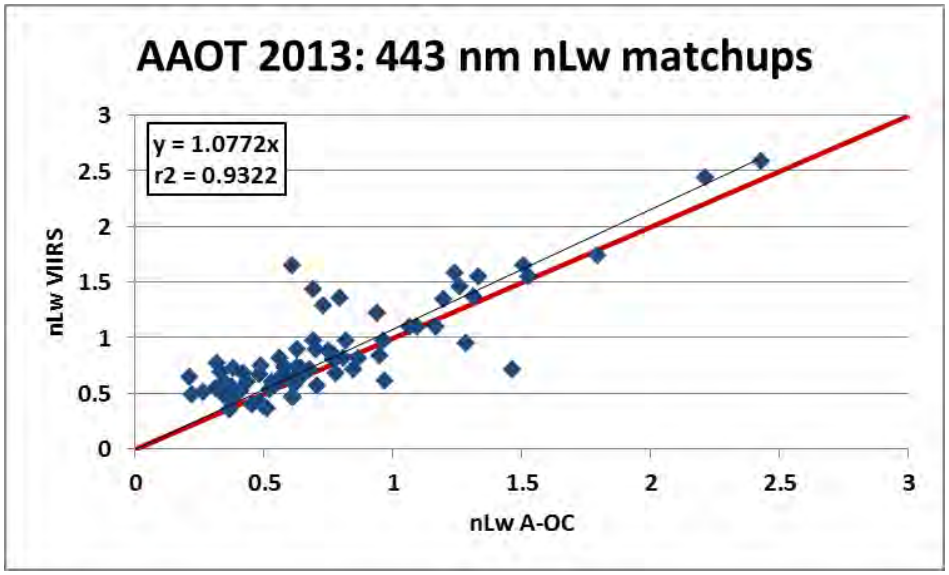

Figure 5 shows the 443 nm nLw matchups for the Venice AERONET site (AAOT/Venise) from 1 Jan 2013 up to 31 Oct 2013. Matchups are the AERONET-OC location to the single pixel from VIIRS. Matchups are minimally screened, removing: negative values at any wavelength, extreme viewing angles, clouds, navigation failures, atmospheric failures. A red 1:1 line is provided for reference. The regression indicates a tight correlation as the VIIRS nLw is 1.07% of the *in situ* value. While the correlation coefficient of the 443 nm relationship indicates 93% of the variation in VIIRS is explained by the variation in the AERONET-OC measurement.

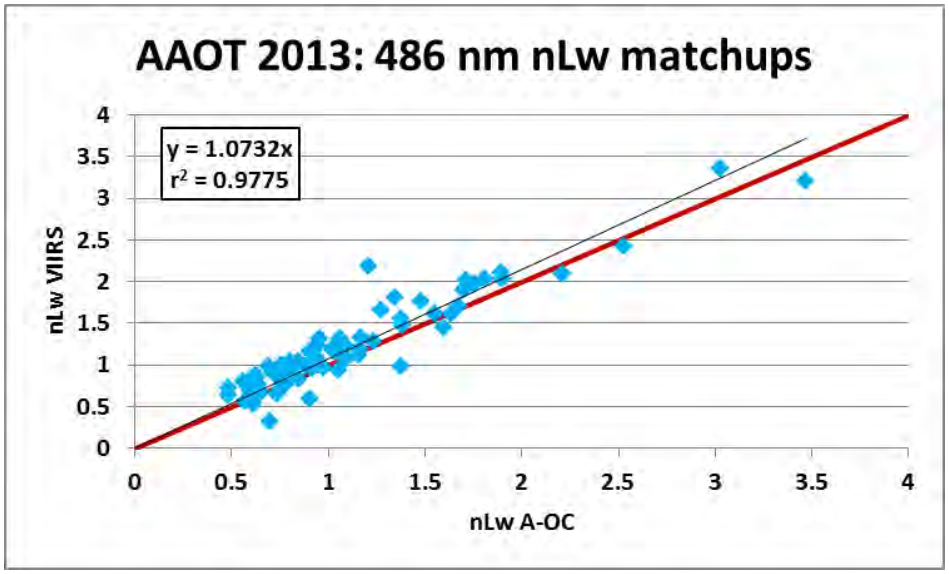

Figure 6 shows the 486 nm nLw matchups for the Venice AERONET site (AAOT/Venise) from 1 Jan 2013 up to 31 Oct 2013. Matchups are the AERONET-OC location to the single pixel from VIIRS. Matchups are minimally screened, removing: negative values at any wavelength, extreme viewing angles, clouds, navigation failures, atmospheric failures. A red 1:1 line is provided for reference. The regression indicates a tight correlation as the VIIRS nLw is 107% of the *in situ* value. While the correlation coefficient of the 486 nm relationship indicates 98% of the variation in VIIRS is explained by the variation in the AERONET-OC measurement.

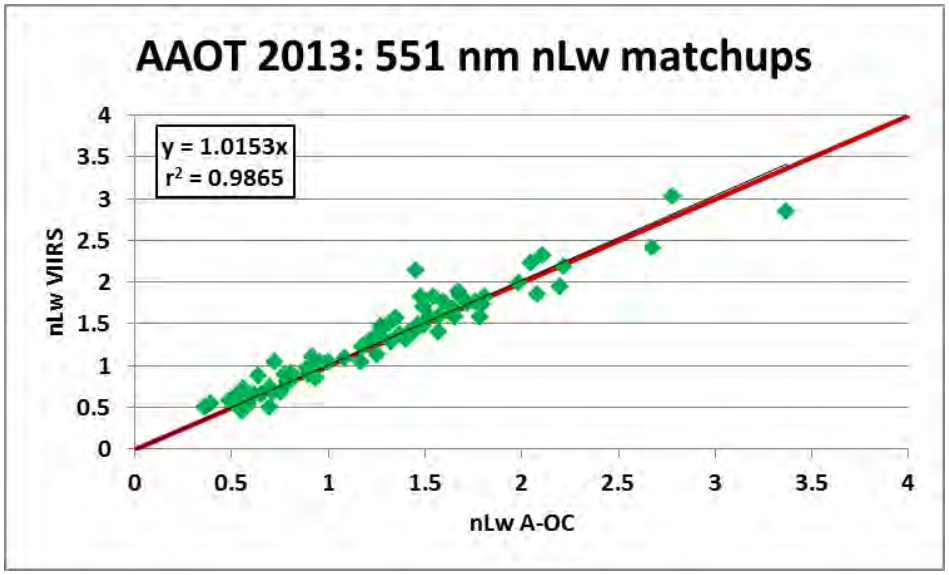

Figure 7 shows the 551 nm nLw matchups for the Venice AERONET site (AAOT/Venise) from 1 Jan 2013 up to 31 Oct 2013. Matchups are the AERONET-OC location to the single pixel from VIIRS. Matchups are minimally screened, removing: negative values at any wavelength, extreme viewing angles, clouds, navigation failures, atmospheric failures. A red 1:1 line is provided for reference. The regression indicates a tight correlation as the VIIRS nLw is 102% of the *in situ* value. While the correlation coefficient of the 555 nm relationship indicates 99% of the variation in VIIRS is explained by the variation in the AERONET-OC measurement.

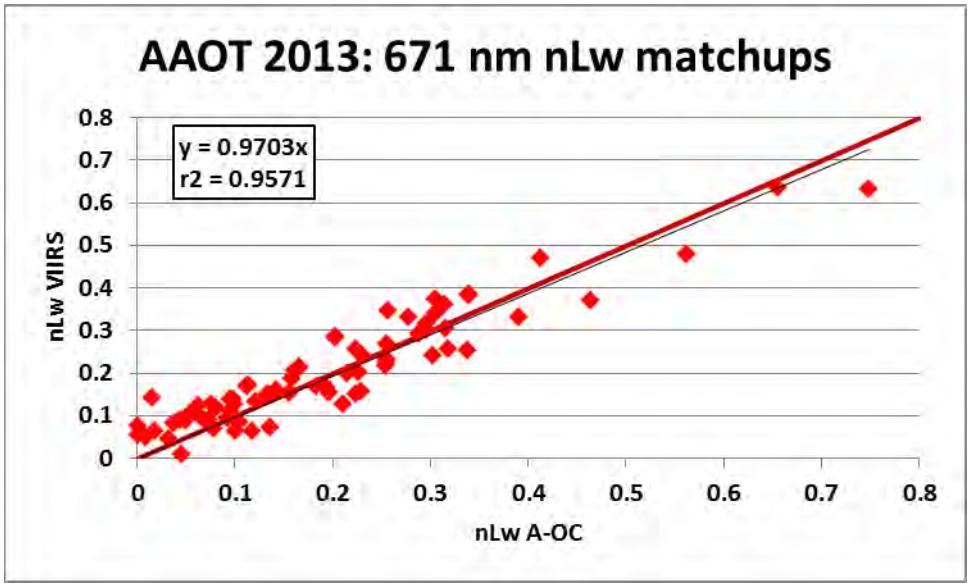

Figure 8 shows the 671 nm nLw matchups for the Venice AERONET site (AAOT/Venise) from 1 Jan 2013 up to 31 Oct 2013. Matchups are the AERONET-OC location to the single pixel from VIIRS. Matchups are minimally screened, removing: negative values at any wavelength, extreme viewing angles, clouds, navigation failures, atmospheric failures. A red 1:1 line is provided for reference. The regression indicates a tight correlation as the VIIRS nLw is 97% of the *in situ* value. While the correlation coefficient of the 671 nm relationship indicates 96% of the variation in VIIRS is explained by the variation in the AERONET-OC measurement.

Table 1 summarizes the statistics for the comparisons between the Venice AERONET AOC and the MODIS sensor for the available 2013 data. The relationships show there is a linear and consistent relationship between the two sensors.

Sensor pairing and Wavelength	slope	r2
AOC:MODIS 412	0.9455	0.8564
AOC:MODIS 442	1.0225	0.9306
AOC:MODIS 488	0.9465	0.9786
AOC:MODIS 532	0.9622	0.9823

Figure 9 and Figure 10 show comparisons between MODIS and VIIRS nLw for 443 nm and 551 nm. In an effort to minimize geometric and biological variability, a mean was computed around the AERONET-OC location using a 3 km x 3 km box size. The linearity and strong correlations shown by these relationships suggest a cross platform calibration at the TOA should be possible as the SDR calibration of VIIRS stabilizes and adequate matchups are assembled. Given the application of vicarious gains to the SDR in July 2013, the accumulation period is not as mature as we had previously believed. We will provide updates in monthly progress reports as the data becomes available.

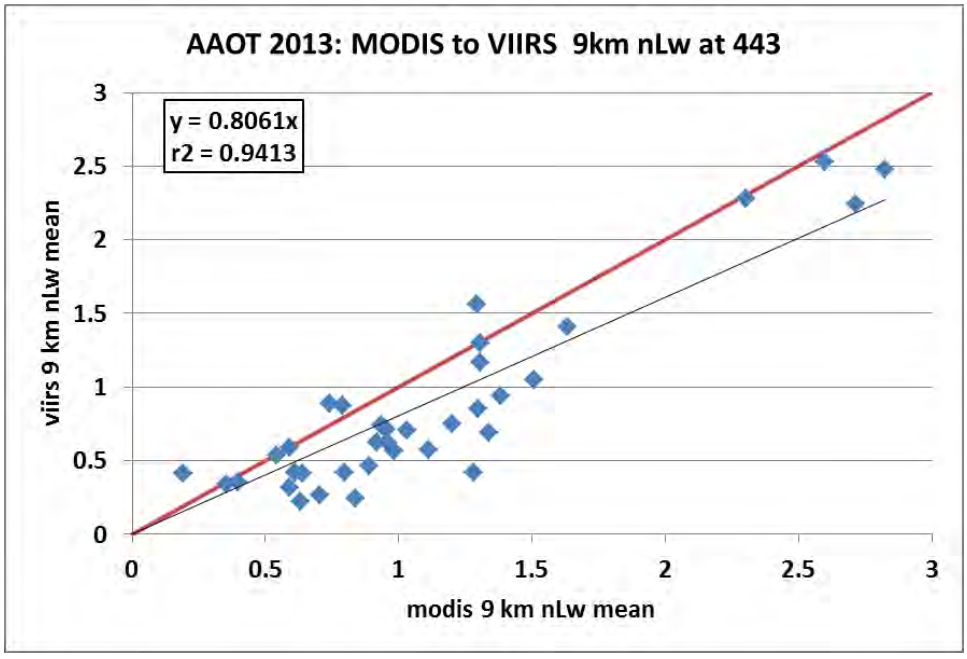

Figure 9 shows the comparison between the MODIS and VIIRS nLw at 443 nm. In an effort to minimize geometric, and biological variability, a mean was computed around the AERONET-OC location using a 3 km x 3 km box size. A red 1:1 line is provided for reference. The regression indicates a high correlation as the VIIRS nLw is 81% of the MODIS value. While the correlation coefficient of the 443 nm relationship indicates 94% of the variation in VIIRS is explained by the variation in the MODIS measurement.

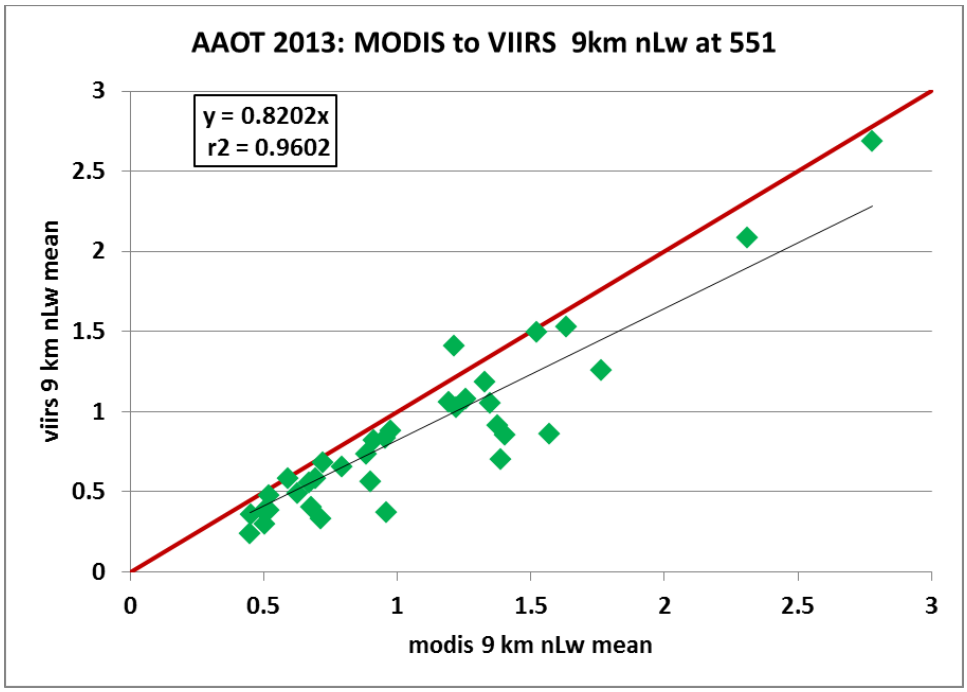

Figure 10 shows the comparison between the MODIS and VIIRS nLw at 551 nm. In an effort to minimize geometric, and biological variability, a mean was computed around the AERONET-OC location using a 3 km x 3 km box size. A red 1:1 line is provided for reference. The regression indicates a high correlation as the VIIRS nLw is 82% of the MODIS value. While the correlation coefficient of the 443 nm relationship indicates 96% of the variation in VIIRS is explained by the variation in the MODIS measurement.

3.2 VIIRS Comparisons to MODIS

Beyond traditional ground truth techniques, NPP ocean color products can be evaluated by direct comparison with existing satellite products such as MODIS. This enables cross-platform capabilities and the technique will rapidly provide consistent data sets from which global metrics of ocean color products can be defined. An additional advantage is that it will provide validation of products in critical coastal regions where *in situ* data is not available yet the VIIRS-MODIS comparison are statistically robust. For the following figures, AOPS v 4.10 is used to generate standard operational products from MODIS and VIIRS for validation comparison purposes.

Figure 11 shows the comparison of VIIRS an MODIS in the Korean Peninsula, March 5, 2013. Three stations were selected from the image to make direct comparison between the sensors in variable water conditions: clear, turbid and transitional. The remote sensing reflectance is directly compared in the embedded graph showing very good agreement of the primary ocean color product in all three water types. Figure 12 shows the same type of comparison for waters in the Persian Gulf, December 9, 2012. These figures indicate the sensor preforms reasonably in different environments.

Korean Peninsula – March 5, 2013 –MODIS vs VIIRS
AOPS v4.10

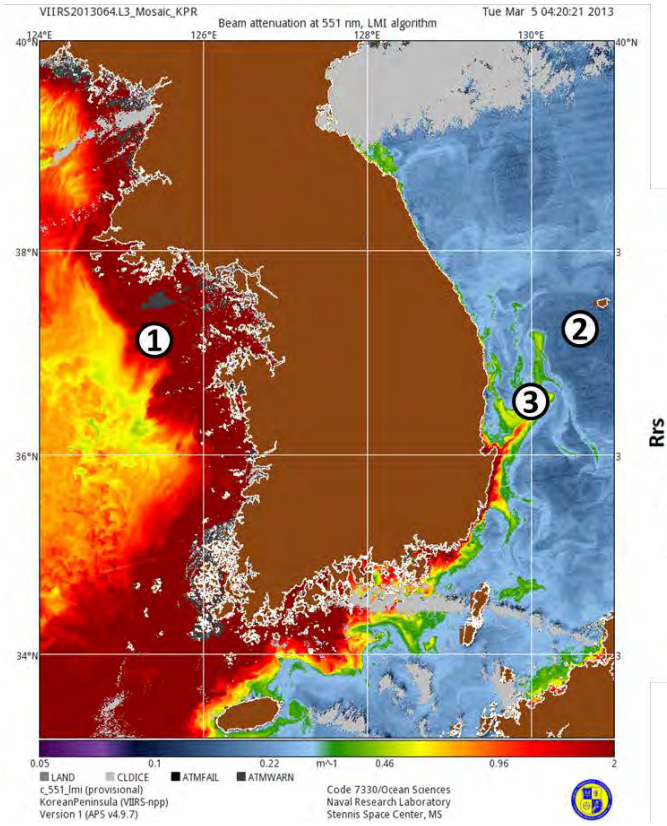

VIIRS(gains) vs, MODIS Rrs improvement at stations 2 & 3 in comparison to MODIS

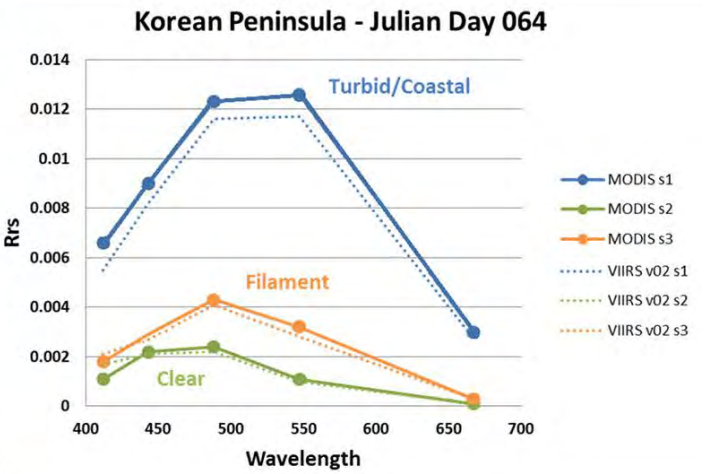

Figure 11*(left)* is a VIIRS image showing three stations around the Korean Peninsula. These stations were chosen to represent variable optical conditions including: 1) turbid water, 2) a transitional zone in a filament, and 3) clear conditions. The graph (*right*) shows the spectral remote sensing reflectance of MODIS *(solid line)* and VIIRS (*dotted line*) at the three stations. VIIRS imagery was processed using AOPS 4.10 with the vicarious calibration (*gains applied*). The sensors agree very well given the data collection is not simultaneous and the 4.10 processing capability with vicarious calibration provides improvement as it compares well with MODIS.

Persian Gulf – December 09, 2012 – MODIS vs VIIRS

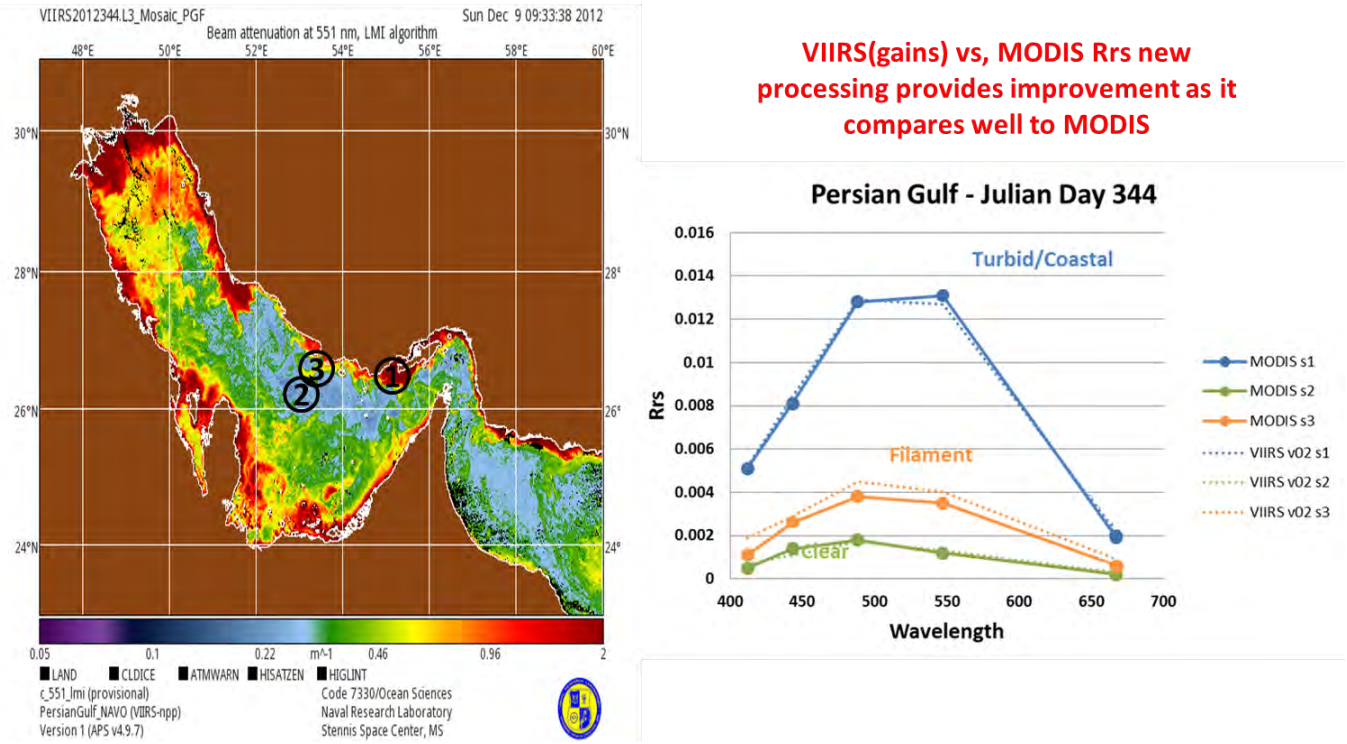

Figure 12 *(left)* is a VIIRS image showing three stations in the Persian Gulf. These stations were chosen to represent variable optical conditions including: 1) turbid water, 2) clear water and 3) a transitional zone. The graph (*right*) shows the spectral remote sensing reflectance of MODIS *(solid line)* and VIIRS (*dotted line*) at the three stations. VIIRS imagery was processed using AOPS 4.10 with the vicarious calibration (*gains applied*). The blue line represents the turbid coats waters. The orange indicates the transitional station and the green represents clear waters. For all three stations, MODIS is denoted by the solid line and VIIRS dotted. The sensors agree very well given the data collection is not simultaneous and the 4.10 processing capability with vicarious calibration provides improvement as it compares well with MODIS.

3.3 Inherent Optical Properties and follow on products

Inherent optical properties and other follow on products are derived from the remote sensing reflectance and water leaving radiance products. Generally there are two accepted approaches for extracting bio-geophysical information from remotely sensed data. Empirical algorithms generally use waveband ratios of upwelling or normalized water-leaving radiance or remote sensing reflectance. Coefficients for these algorithms are generally derived by global and seasonal pooling of data collected at a variety of temporal and spatial scales. This approach removes "noise" associated with the data sets but diminishes the spatial and temporal features of the global waters. Alternatively semi-analytical algorithms are based on the spectral $b_b/(a+b_b)$ to remote sensing reflectance relationship. By taking a physics based

approach, improved products will become available however it is important to recognize development of these algorithms remains a work in progress.

It is important to note for the general oceanographer not familiar with optics, IOP retrievals are difficult and can reflect the limitations of the algorithms rather than stand as a statement regarding satellite performance. A through discussion of deriving IOPS from remote sensing can be found in the IOCCG Report 5, 2006. As algorithm development is outside the scope of this work, figures presented here will illustrate the VIIRS IOP matchups with a variety of sources. As a baseline, literature suggests that mean relative errors ranging from 30 – 70% for IOP retrievals are not uncommon in coastal waters (Chang and Gould, 2006, Ladner, et al 2002).

Figure 13 through Figure 20 show comparisons between the VIIRS and MODIS spectral absorption and attenuation coefficients in the Korean Peninsula and Persian Gulf. A turbid water and clear water station were selected for each site. The data show reasonable results.

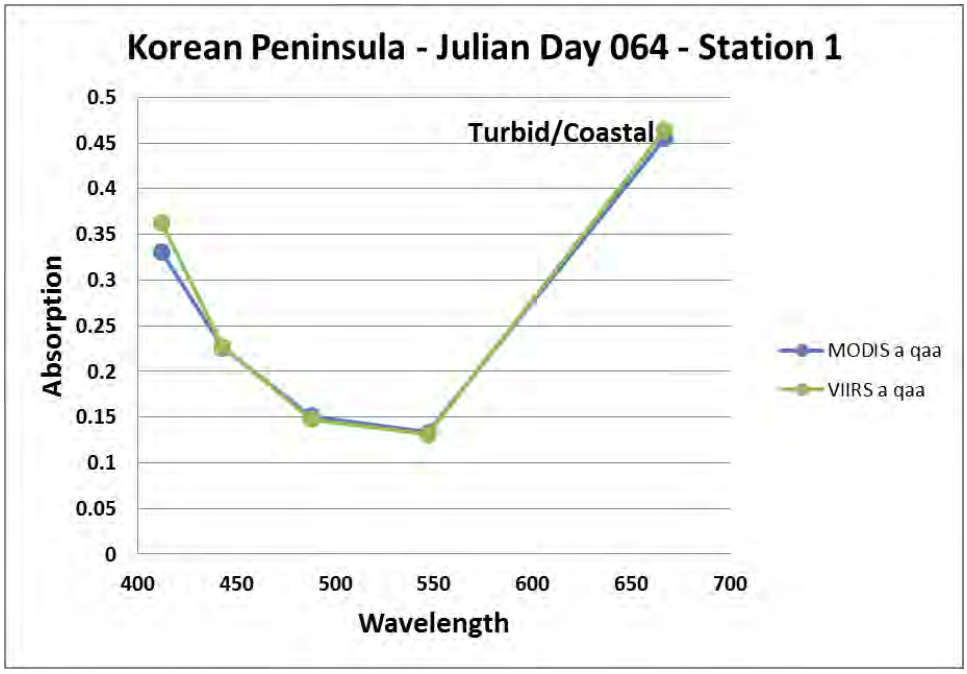

Figure 13 compares the spectral absorption product from the turbid water station (#1) from the Korean Peninsula image, Figure 11. The QAA semi-analytical algorithm was used on both MODIS (blue) and VIIRS (green) same day imagery.

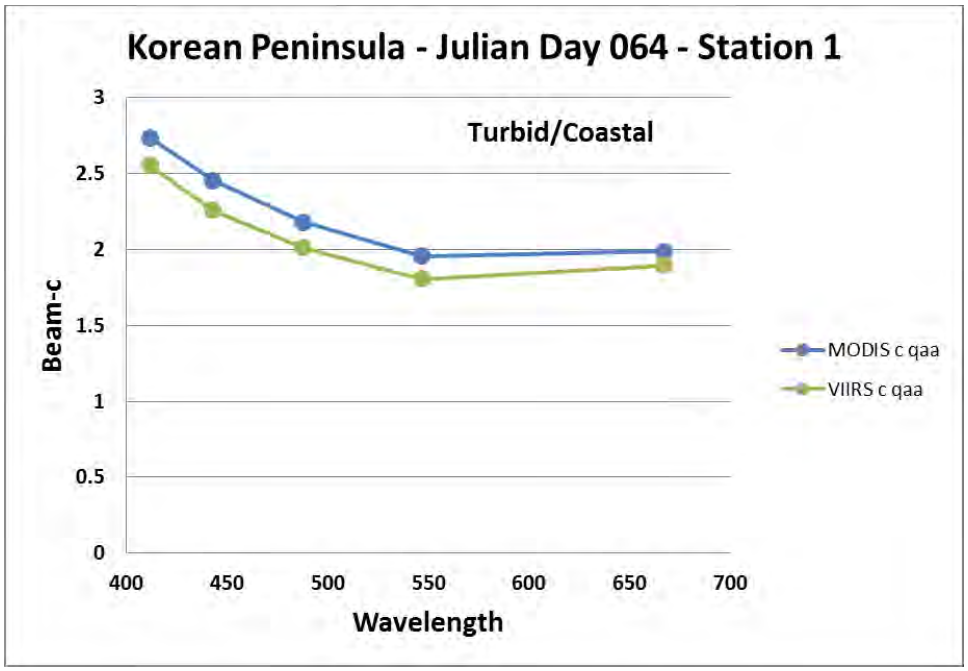

Figure 14 compares the spectral beam attenuation product from the turbid water station (#1) from the Korean Peninsula image, Figure 11. The QAA semi-analytical algorithm was used on both MODIS (blue) and VIIRS (green) same day imagery.

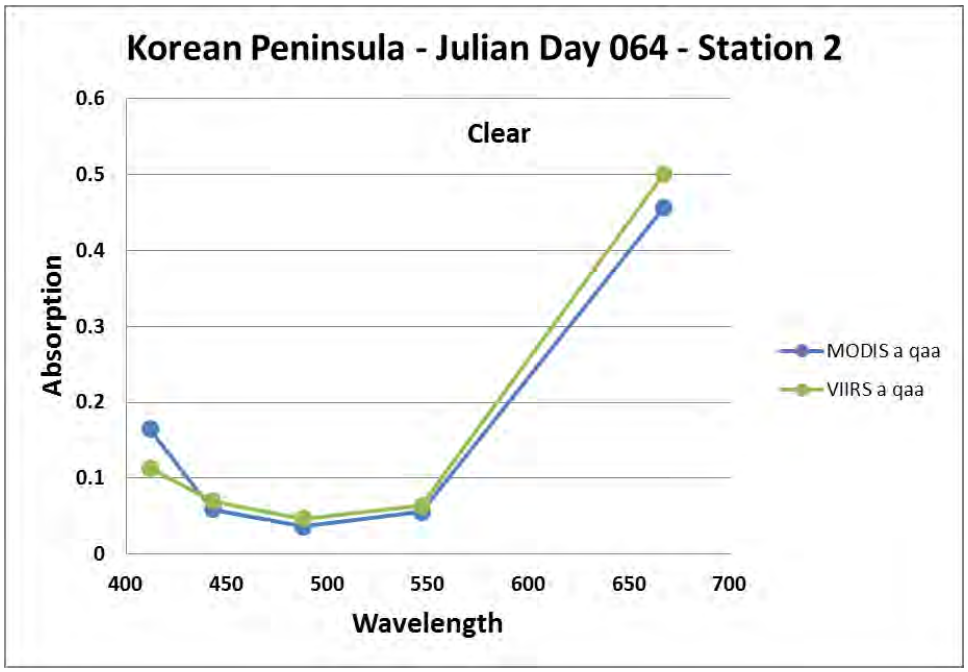

Figure 15 compares the spectral absorption product from the clear water station (#2) from the Korean Peninsula image, Figure 11. The QAA semi-analytical algorithm was used on both MODIS (blue) and VIIRS (green) same day imagery.

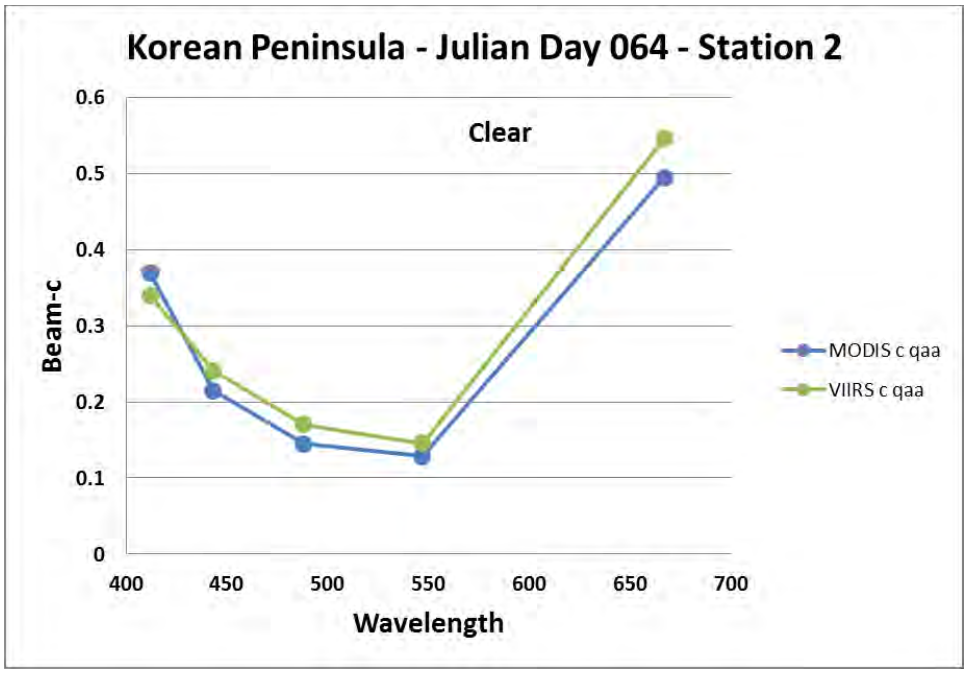

Figure 16 compares the spectral attenuation products from the clear water station (#2) from the Korean Peninsula image, Figure 11. The QAA semi-analytical algorithm was used on both MODIS (blue) and VIIRS (green) same day imagery.

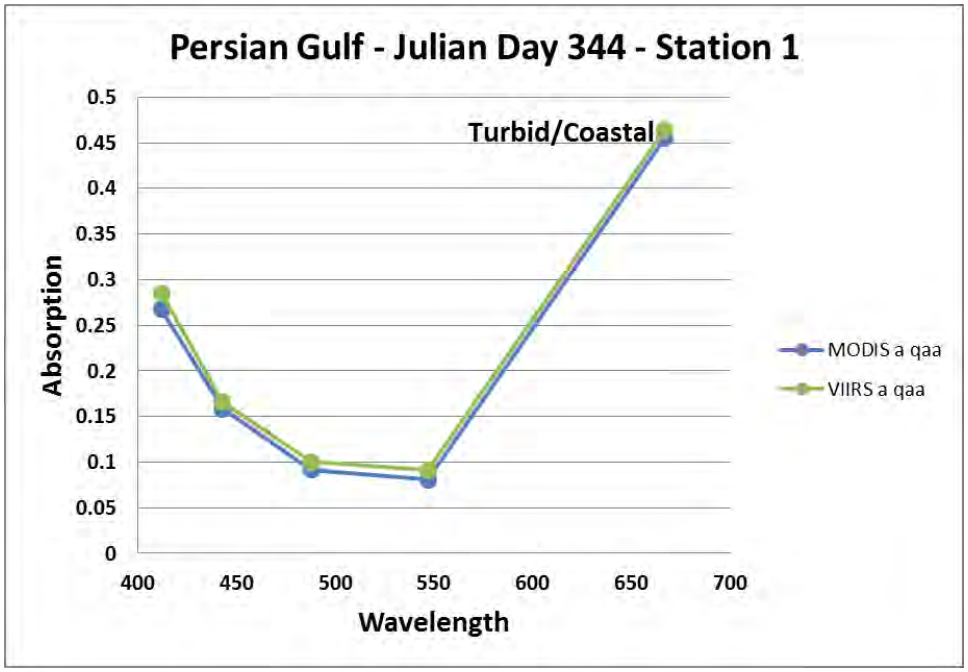

Figure 17 compares the spectral absorption products from the turbid water station (#1) from the Persian Gulf image, Figure 12Figure 11. The QAA semi-analytical algorithm was used on both MODIS (blue) and VIIRS (green) same day imagery.

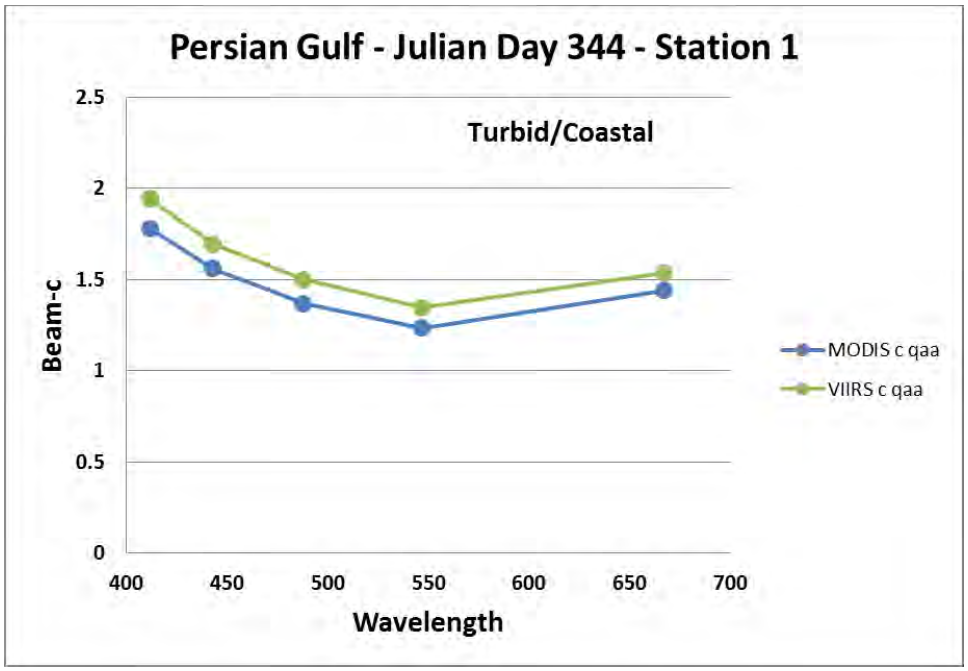

Figure 18 compares the spectral attenuation products from the turbid water station (#1) from the Persian Gulf image, Figure 12Figure 11. The QAA semi-analytical algorithm was used on both MODIS (blue) and VIIRS (green) same day imagery.

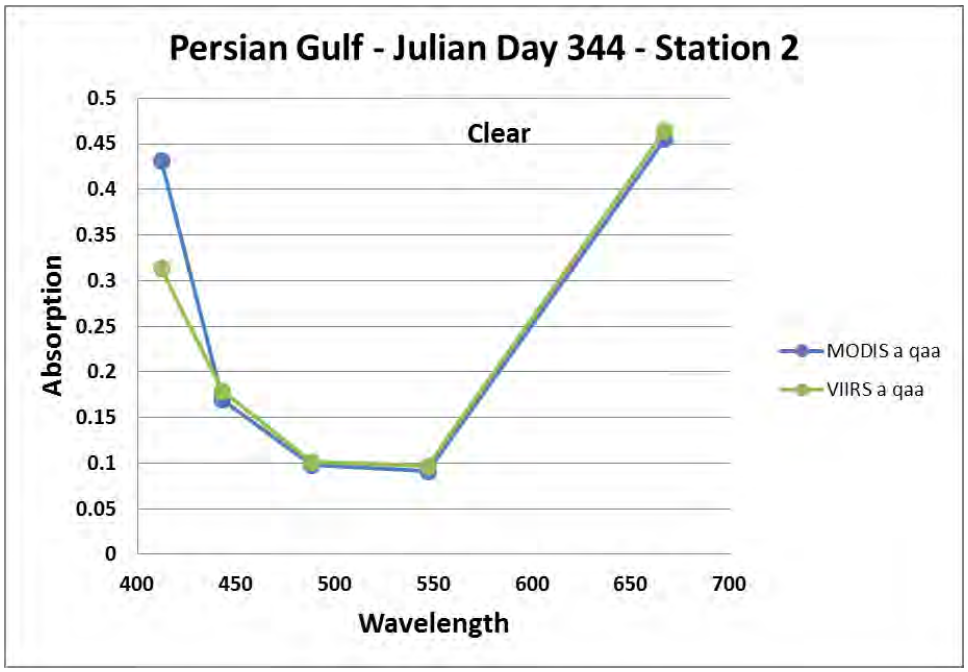

Figure 19 compares the spectral absorption products from the clear water station (#1) from the Persian Gulf image, Figure 12Figure 11. The QAA semi-analytical algorithm was used on both MODIS (blue) and VIIRS (green) same day imagery.

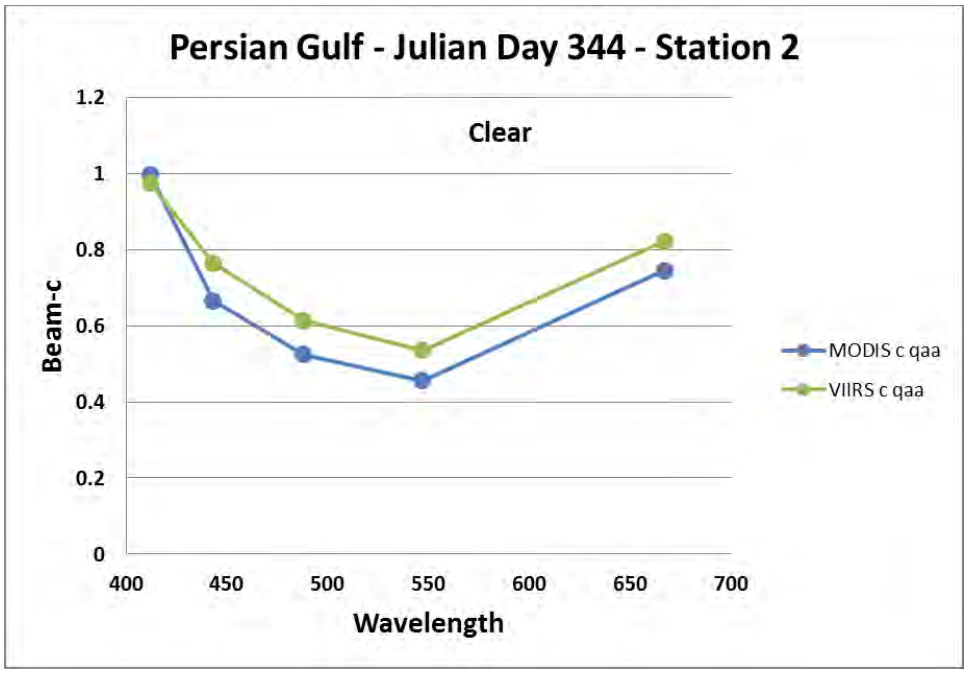

Figure 20 compares the spectral attenuation products from the clear water station (#2) from the Persian Gulf image, Figure 12Figure 11. The QAA semi-analytical algorithm was used on both MODIS (blue) and VIIRS (green) same day imagery.

Data was collected as cruise support for the NASA GEOstationary Coastal and Air Pollution Events (GEO-CAPE) mission and provided to NRL courtesy of Mike Ondrusek and Zhongping Lee. AOP and IOP data were collected using a variety of instrumentation including surface measurements, profiling packages and a flow-through system. Figure 21 shows the VIIRS derived total backscatter product to support the NASA/NOAA GEOCAPE cruise that took place in the Northern Gulf of Mexico from July 9 to the 19, 2013. Station locations are dotted in blue.

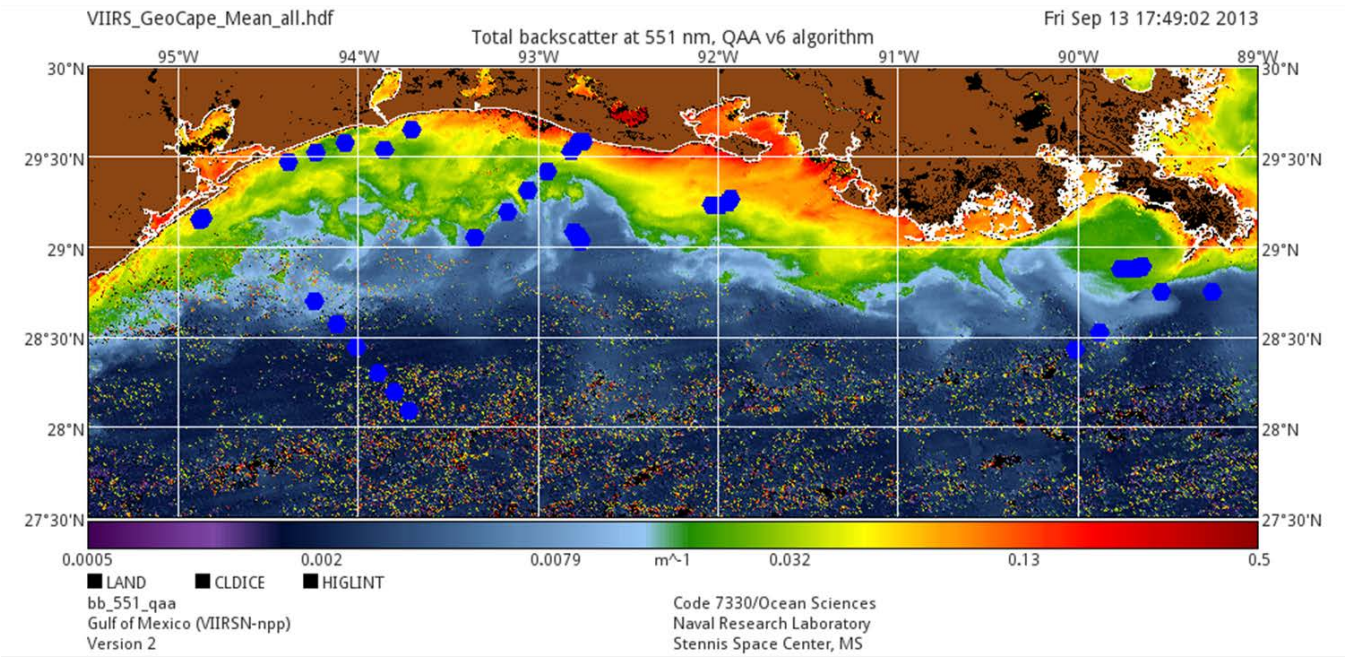

Figure 21 shows the VIIRS derived total backscatter product to support the NASA/NOAA GEOCAPE cruise that took place in the Northern Gulf of Mexico from July 9 to the 19, 2013. Station locations are dotted in blue.

Figure 22 through Figure 29 show the spectral absorption and attenuation product comparisons between VIIRS, MODIS and the ac-9. A strong linear relationship is seen at all wavelengths. Discrepancies are attributed to inadequacies in atmospheric corrections, particularly at blue wavelengths, and uncertainties originating from sampling errors related to pixel to point comparisons as well as the natural temporal and spatial variability prevalent in the coastal waters. Regression results of optical properties in coastal waters have been reported to have errors ranging from 30 to 70% (Chang, et al, Ladner, et al). Further improvements between satellite and *in situ* data may be possible with future algorithm development.

Figure 22 shows the 412 nm absorption coefficient matchups between the AOPS v 4.10 processed satellite imagery and the *in situ* data collection from the GEOCAPE cruise. MODIS and VIIRS agree well with one another and are both approximately 20% higher than the *in situ* absorption measurement taken with an *ac-9*.

Figure 23 shows the 443 nm absorption coefficient matchups between the AOPS v 4.10 processed satellite imagery and the *in situ* data collection from the GEOCAPE cruise. MODIS and VIIRS agree

well with one another and are both approximately 20% higher than the *in situ* absorption measurement taken with an *ac-9*.

Figure 24 shows the 488 nm absorption coefficient matchups between the AOPS v 4.10 processed satellite imagery and the *in situ* data collection from the GEOCAPE cruise. The MODIS absorption product at this wavelength is approximately 7% too low as compared to the *ac-9* measurement. The VIIRS absorption retrieval performs well in this case at this wavelength.

Figure 25 shows the 547 nm absorption coefficient matchups between the AOPS v 4.10 processed satellite imagery and the *in situ* data collection from the GEOCAPE cruise. MODIS and VIIRS both show a liner response. The MODIS absorption retrieval performs well where VIIRS is approximately 10% to high.

Figure 26 shows the 412 nm beam attenuation coefficient matchups between the AOPS v 4.10 processed satellite imagery and the *in situ* data collection from the GEOCAPE cruise. MODIS absorption is approximately 40% too low compared to the *ac-9* where VIIRS is approximately 10% low. Important to note for the general oceanographer not familiar with optics, IOP retrievals are difficult and can reflect the limitations of the algorithms rather than stand as a statement regarding satellite performance.

Figure 27 shows the 443 nm beam attenuation coefficient matchups between the AOPS v 4.10 processed satellite imagery and the *in situ* data collection from the GEOCAPE cruise. MODIS is approximately 50% too low as compared to the *ac-9* where VIIRS is approximately 27% to low. Important to note for the general oceanographer not familiar with optics, IOP retrievals are difficult and can reflect the limitations of the algorithms rather than stand as a statement regarding satellite performance.

Figure 28 shows the 488 nm beam attenuation coefficient matchups between the AOPS v 4.10 processed satellite imagery and the *in situ* data collection from the GEOCAPE cruise. MODIS is approximately 52% too low as compared to the *ac-9* where VIIRS is approximately 32% to low.

Figure 29 shows the 547 nm beam attenuation coefficient matchups between the AOPS v 4.10 processed satellite imagery and the *in situ* data collection from the GEOCAPE cruise. MODIS is approximately 54% too low as compared to the *ac-9* where VIIRS is approximately 33% to low.

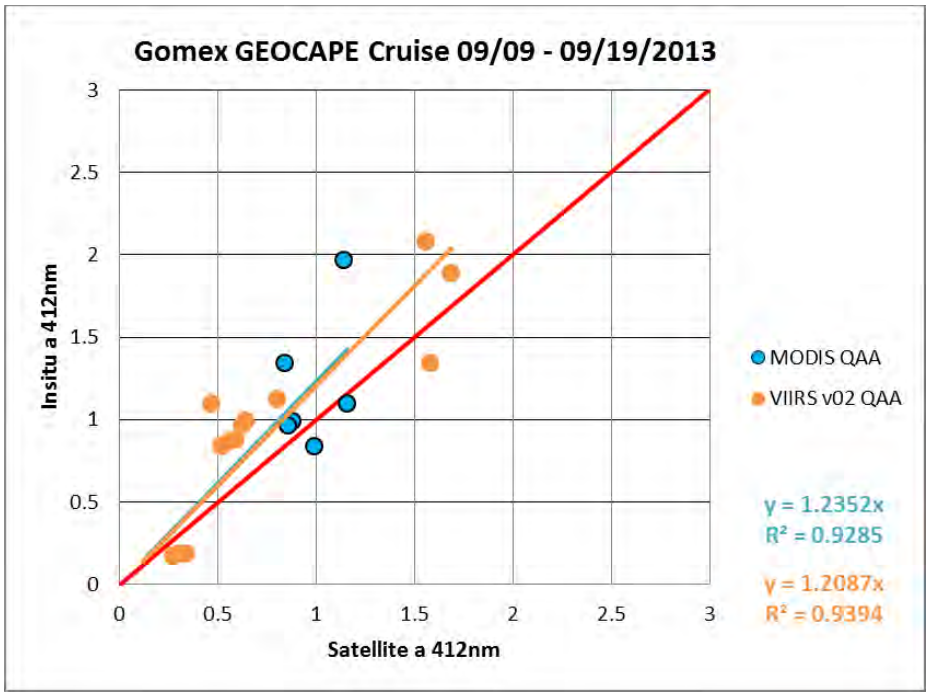

Figure 22 shows the 412 nm absorption coefficient matchups between the AOPS v 4.10 processed satellite imagery and the *in situ* data collection from the GEOCAPE cruise. MODIS and VIIRS agree well with one another and are both approximately 20% higher than the *in situ* absorption measurement taken with an *ac-9*.

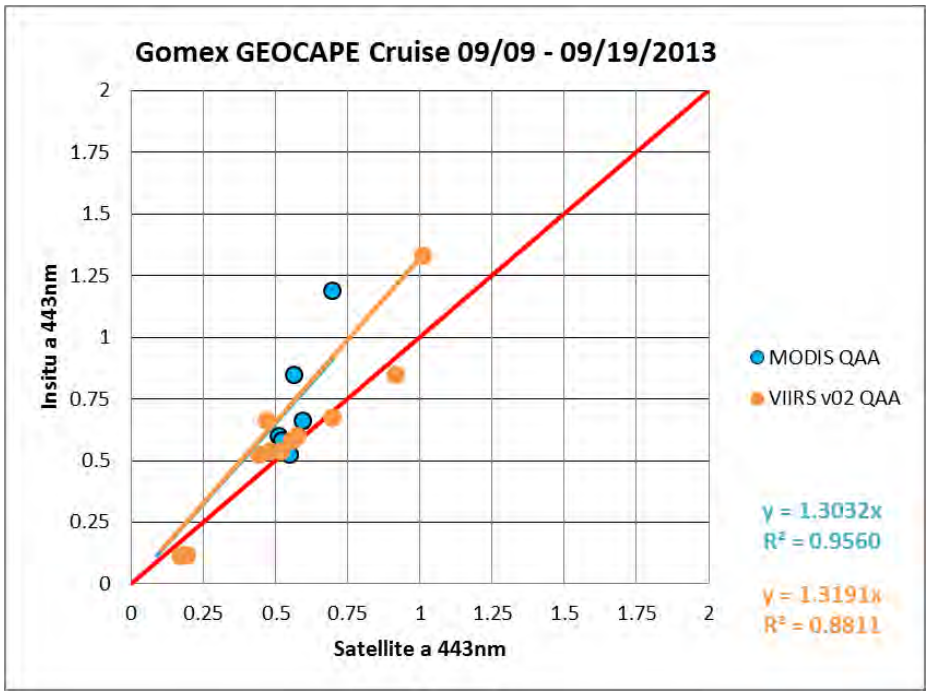

Figure 23 shows the 443 nm absorption coefficient matchups between the AOPS v 4.10 processed satellite imagery and the *in situ* data collection from the GEOCAPE cruise. MODIS and VIIRS agree well with one another and are both approximately 20% higher than the *in situ* absorption measurement taken with an *ac-9*.

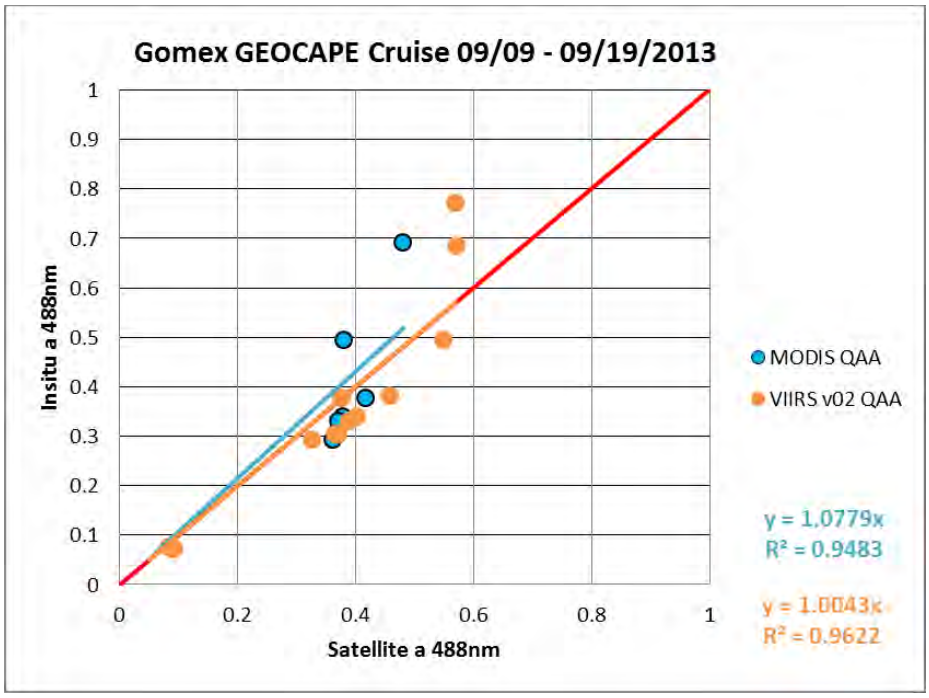

Figure 24 shows the 488 nm absorption coefficient matchups between the AOPS v 4.10 processed satellite imagery and the *in situ* data collection from the GEOCAPE cruise. The MODIS absorption product at this wavelength is approximately 7% too low as compared to the *ac-9* measurement. The VIIRS absorption retrieval performs well in this case at this wavelength.

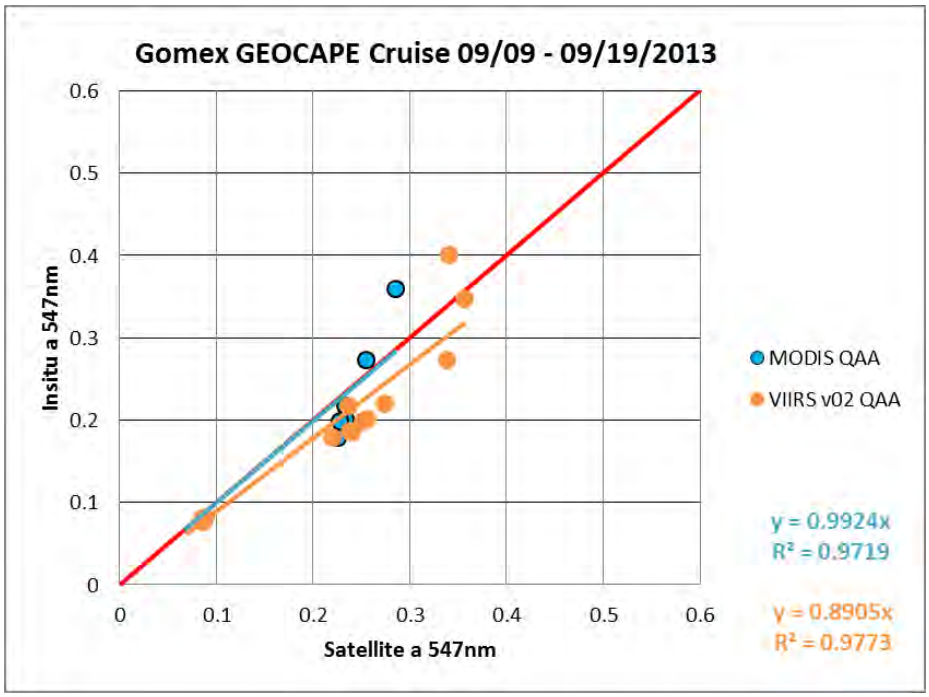

Figure 25 shows the 547 nm absorption coefficient matchups between the AOPS v 4.10 processed satellite imagery and the *in situ* data collection from the GEOCAPE cruise. MODIS and VIIRS both show a liner response. The MODIS absorption retrieval performs well where VIIRS is approximately 10% to high.

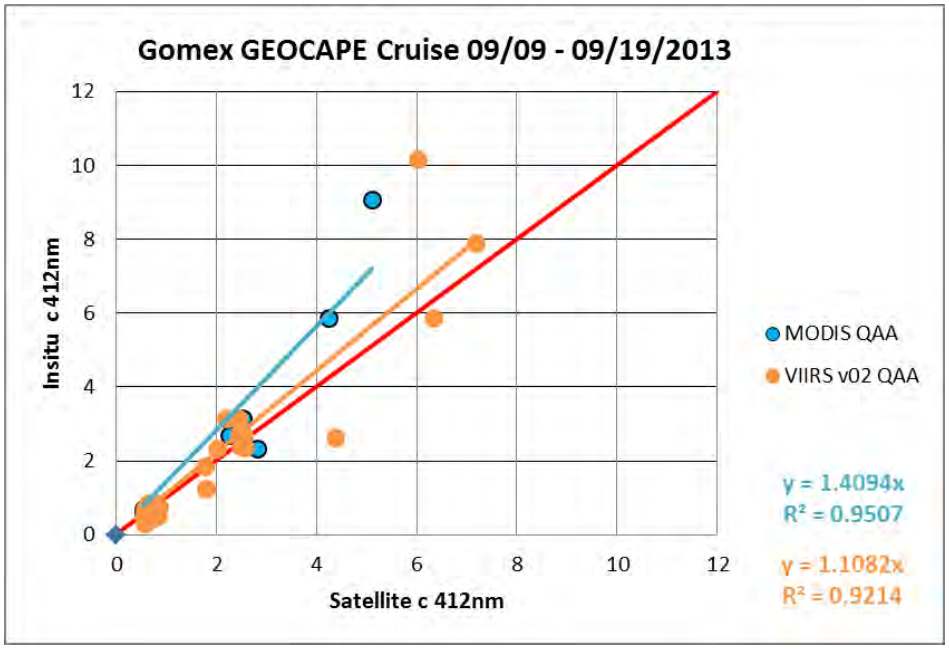

Figure 26 shows the 412 nm beam attenuation coefficient matchups between the AOPS v 4.10 processed satellite imagery and the *in situ* data collection from the GEOCAPE cruise. MODIS absorption is approximately 40% too low compared to the *ac-9* where VIIRS is approximately 10% low. Important to note for the general oceanographer not familiar with optics, IOP retrievals are difficult and can reflect the limitations of the algorithms rather than stand as a statement regarding satellite performance.

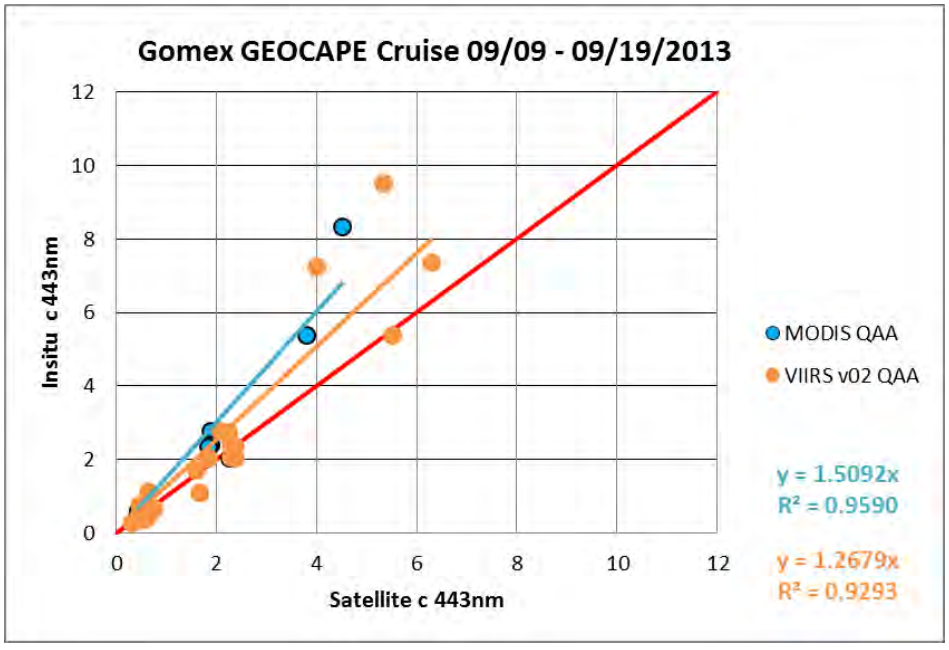

Figure 27 shows the 443 nm beam attenuation coefficient matchups between the AOPS v 4.10 processed satellite imagery and the *in situ* data collection from the GEOCAPE cruise. MODIS is approximately 50% too low as compared to the *ac-9* where VIIRS is approximately 27% to low. Important to note for the general oceanographer not familiar with optics, IOP retrievals are difficult and can reflect the limitations of the algorithms rather than stand as a statement regarding satellite performance.

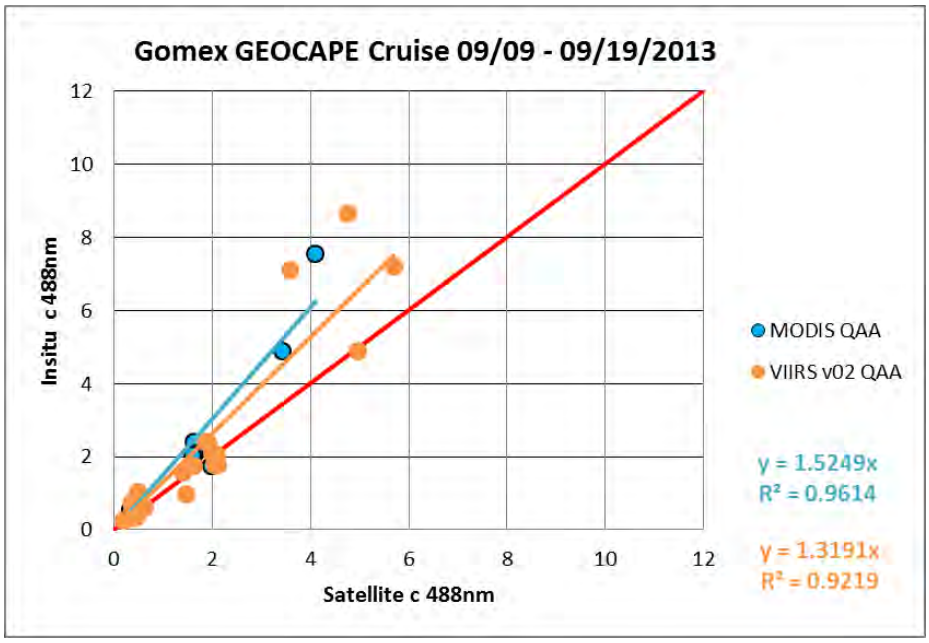

Figure 28 shows the 488 nm beam attenuation coefficient matchups between the AOPS v 4.10 processed satellite imagery and the *in situ* data collection from the GEOCAPE cruise. MODIS is approximately 52% too low as compared to the *ac-9* where VIIRS is approximately 32% to low.

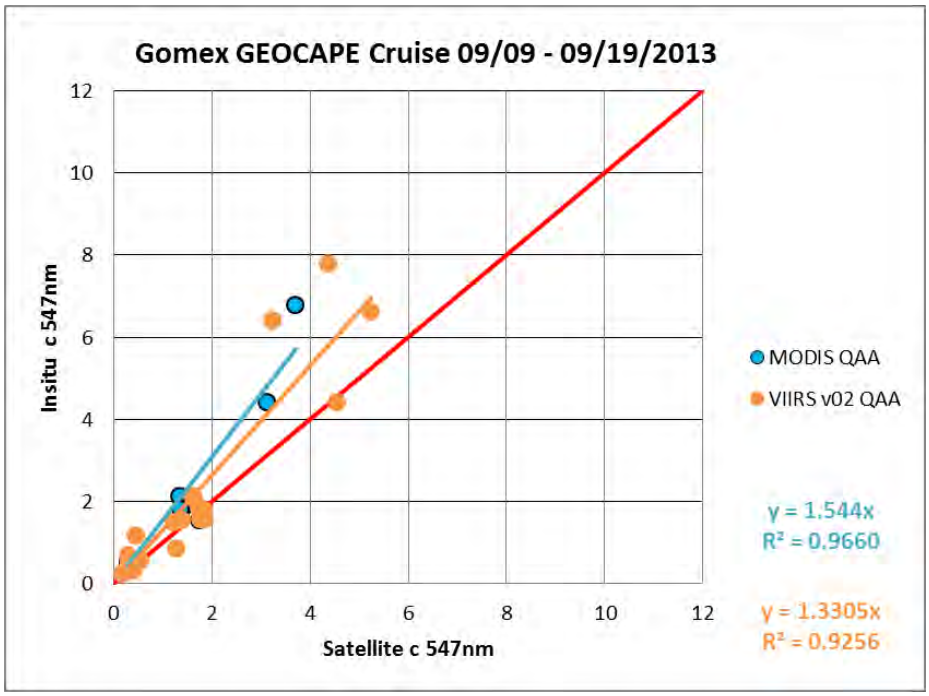

Figure 29 shows the 547 nm beam attenuation coefficient matchups between the AOPS v 4.10 processed satellite imagery and the *in situ* data collection from the GEOCAPE cruise. MODIS is approximately 54% too low as compared to the *ac-9* where VIIRS is approximately 33% to low.

Table 2 summarizes the statistics for the remote sensing reflectance matchups between VIIRS and MODIS for the GEOCAPE cruise. This table shows the v02 (AOPS v4.10) including vicariously calibrated gains derived from MOBY is an improvement over the v01 (AOPS v4.8) processing using unity gains and performs well (closeness to 1 and high r^2) at several wavelengths.

Slope	rrs412	rrs443	rrs488	rrs547	rrs667
MODIS	0.85	0.82	0.94	1.07	1.18
VIIRS v01	0.5	0.72	0.85	0.91	0.79
VIIRS v02	0.79	0.91	0.97	0.99	0.85

r^2	rrs412	rrs443	rrs488	rrs547	rrs667
MODIS	0.9852	0.9800	0.9692	0.9713	0.9720
VIIRS v01	0.9059	0.9668	0.9841	0.9826	0.9582
VIIRS v02	0.8768	0.9638	0.9801	0.9788	0.9573

An additional cruise aboard the *RV Ocean Color* was conducted on Nov 20, 2013 in which stations and flow-through system data were collected. The flow through data included ac-9 (absorption and beam attenuation) along a path from Bay St Louis out to the Gulf of Mexico. These data were spatially bin averaged to matchup with the retrieved VIIRS ocean products. Figure 30 shows the location of transect data taken from A to B off the coast of Mississippi. The left plot shows the matchup along the track for the IOP – 443 nm absorption products from MODIS and VIIRS using AOPS, VOCCO, and the ac-9 *in situ* measurement. The right plot shows the regression of satellite products against the *in situ* 443 nm products. Note the VOCCO product (using Carter algorithm and derived using the NOAA IDPS without the coastal NIR iteration) has data gaps because of non-retrievals (negative nLw's) in the EDR/L3 product. The MODIS retrievals (red) were above the one to one line. The VIIRS AOPS retrievals with vicariously calibrated gains applied (purple) used the QAA algorithm and coastal NIR processing, all falling close the one to one line (slope = 1.05). Notably, the VIIRS ocean color products are doing better than MODIS in this coastal ocean comparison. *This supports arguments for upgrading the IDPS' IOP algorithms and atmospheric correction (NIR iterative correction) procedure to support coastal ocean products.*

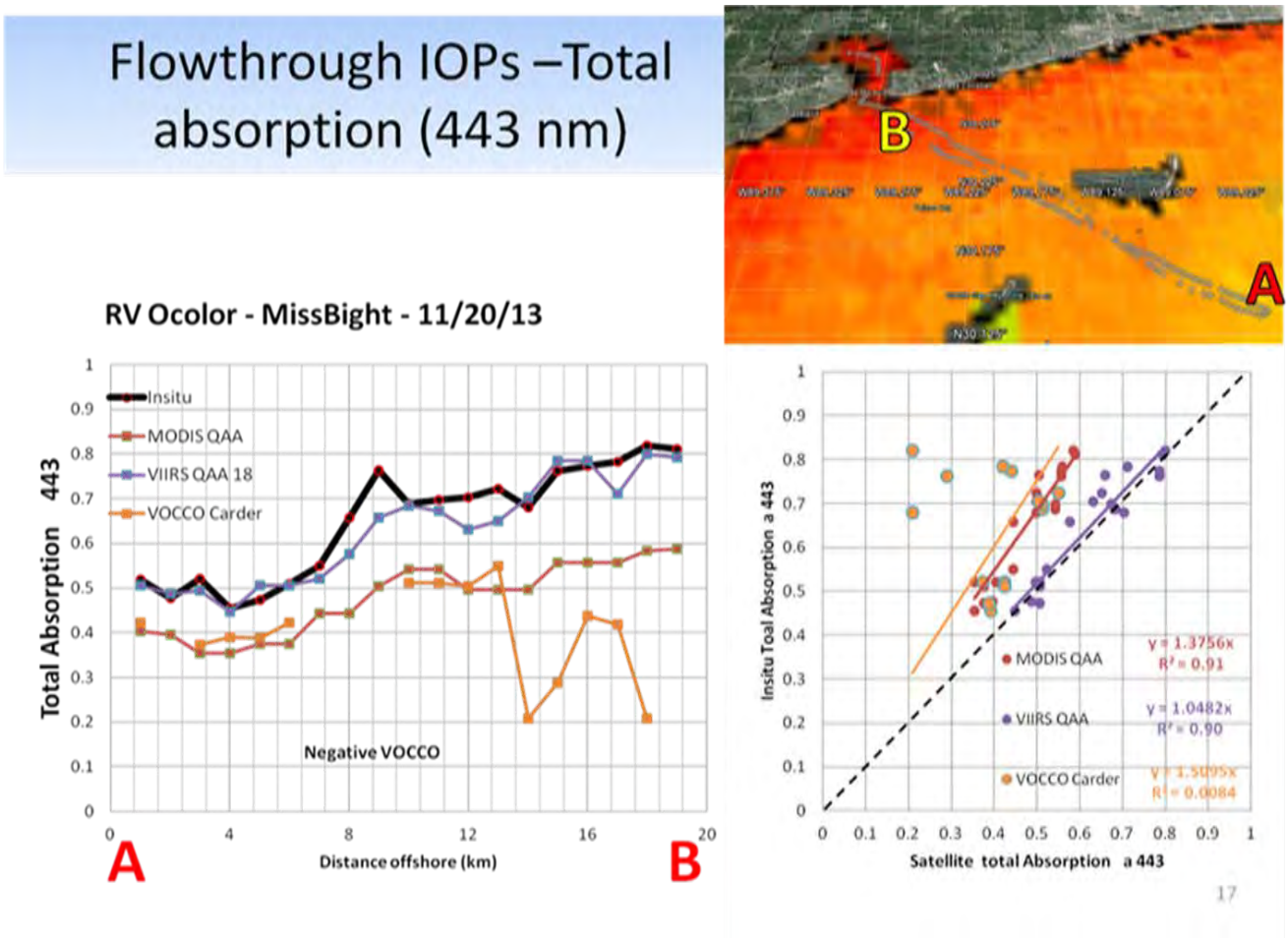

Figure 30 shows the location of transect data taken from A to B off the coast of Mississippi. The left plot shows the matchup along the track for the IOP – 443 nm absorption products from MODIS and VIIRS using AOPS, VOCCO, and the ac-9 *in situ* measurement. The right plot shows the regression of satellite products against the *in situ* 443 nm products. Note the VOCCO product (using Carter algorithm) has data gaps because of non-retrievals (negative nLw's) of the EDR product. The MODIS retrievals (red) were above the one to one line. The VIIRS AOPS retrievals (purple) used the QAA algorithm and NIR processing, all falling close the one to one line (slope = 1.05). Notably, the VIIRS ocean color products are doing better than MODIS in this comparison. *This supports arguments for upgrading the IDPS to support coastal ocean products.*

3.4 GOCI support

To evaluate the current AOPS v 4.10 processing of GOCI level 1b water leaving radiance (nL_w), we provide an inter-sensor comparison between GOCI, MODIS, and VIIRS remote sensing reflectances. This comparison was performed in the East China Sea using AERONET-OC from the Gageocho and Ieodo stations. The MODIS was processed with MOBY gains derived by NASA. The VIIRS was processed with unity and MOBY gains recently derived by NRL. The GOCI was processed with unity and the MODIS – SWIR derived vicarious calibration gains, as defined by Wang, 2012. These gain values are show in Table 3.

The GOCI data from 4Z GMT (*corresponds to local 1:00 pm*) was used to reduce sun glint and sensor issues. Also relevant to this analysis, the Gageocho SeaPrism was moved to Ieodo, resulting in a data gap from May 2012 to Dec 2013 and the AERONET-OC radiance was spectrally shifted to correspond to the GOCI wavelengths.

Table 3 gain values for GOCI bands obtained from Wang (2012).

Band	Gain
412 nm	0.9862
443 nm	0.9753
490 nm	0.9473
555 nm	0.9149
660 nm	0.9245
680 nm	0.9223
745 nm	0.9430
865 nm	1.0000

Figure 31 shows comparisons of the GOCI, VIIRS and MODIS sensors at the Ieodo and Gageocho stations for Julian day 118, 2013. The *in situ* data is the red dashed line. The MODIS data is processed with NASA gains and shown as a black solid line. The VIIRS (NRL gains) and GOCI (NOAA gains) data are represented by solid lines. The VIIRS and GOCI data processed with unity gains (i.e., no gains) is denoted with dashed lines. *Recall the gains are applied at the TOA and subsequent remote sensing reflectance retrievals are a non-linear process.*

Figure 32 shows the spectral comparisons of the GOCI, VIIRS and MODIS sensors at the Gageocho site for Julian day 277, 2013. The MODIS data is processed with gains and shown as a black solid line. The VIIRS and GOCI data processed with gains are represented by solid lines. The VIIRS and GOCI data processed with unity gains (i.e., no gains) is denoted with dashed lines. *In situ* data was unavailable for this comparison. VIIRS and MODIS agree reasonably well with the exception of the 443 nm reflectance which is likely an effect of complex marine atmospheres typical in the coastal regions and the issues that arise with pixel to point comparisons. The GOCI data shows improvement with the gains applied however is higher than MODIS at all wavelengths.

Figure 33 shows the spectral comparisons of the AOC, GOCI, VIIRS and MODIS sensors at the Ieodo station for Julian day 341, 2013. The *in situ* data at Ieodo is provided as the red dashed line. The MODIS data is processed with gains and shown as a black dashed line. The VIIRS and GOCI data processed with gains are represented by solid lines. The VIIRS and GOCI data processed with unity gains (i.e., no gains) is denoted with dashed lines. VIIRS and MODIS agree with regard to spectral shape however, with the gains applied the VIIRS shows lower reflectances at the lower wavelengths as compared to MODIS however VIIRS compares very well with the *in situ* data with a slight discrepancy at 412 nm. The GOCI data provides better retrievals in comparison to both MODIS an AOC without the gains applied. The GOCI without gains agrees better with AOC than MODIS for this date time combination.

Figure 34 shows the time series of remote sensing reflectance at 550 nm for the *in situ* AOC, MODIS,GOCI, and VIIRS sensors. Data are shown for the 4 Zulu time to minimize sun glint and sensor issues. The data and satellite retrievals show good agreement.

Figure 35 shows a visual comparison of GOCI, MODIS and VIIRS backscatter at 551 nm products for Julian day 277. The GOCI and VIIRS products with gains are visually closer to the MODIS product than the products without gains.

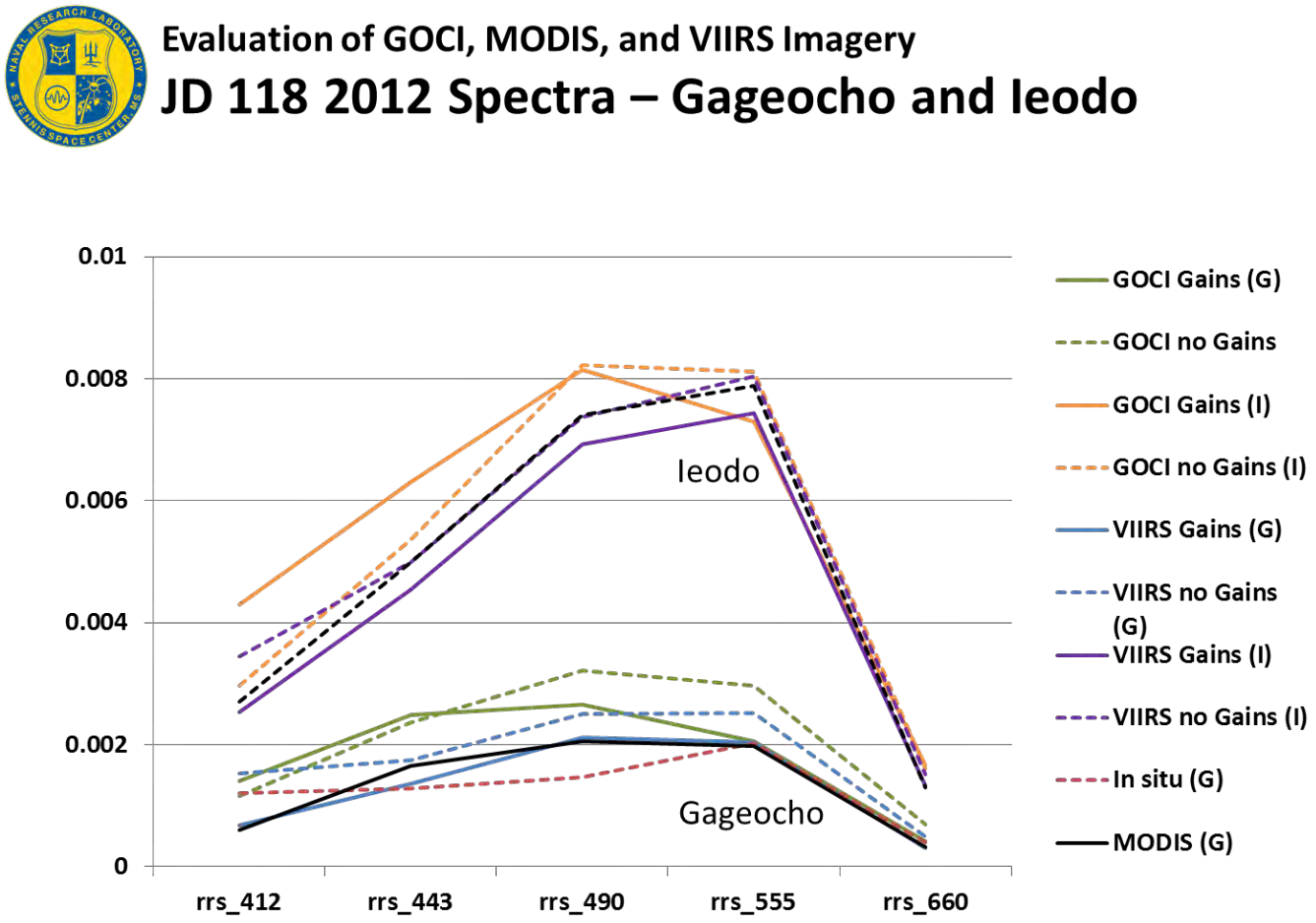

Figure 31 shows comparisons of the GOCI, VIIRS and MODIS sensors at the Ieodo and Gageocho stations for Julian day 118, 2013. The *in situ* data is the red dashed line. The MODIS data is processed with gains and shown as a black solid line. The VIIRS and GOCI data processed with gains are represented by solid lines. The VIIRS and GOCI data processed with unity gains (i.e., no gains) is denoted with dashed lines. *Recall the gains are applied at the TOA and subsequent remote sensing reflectance retrievals are a non-linear process.*

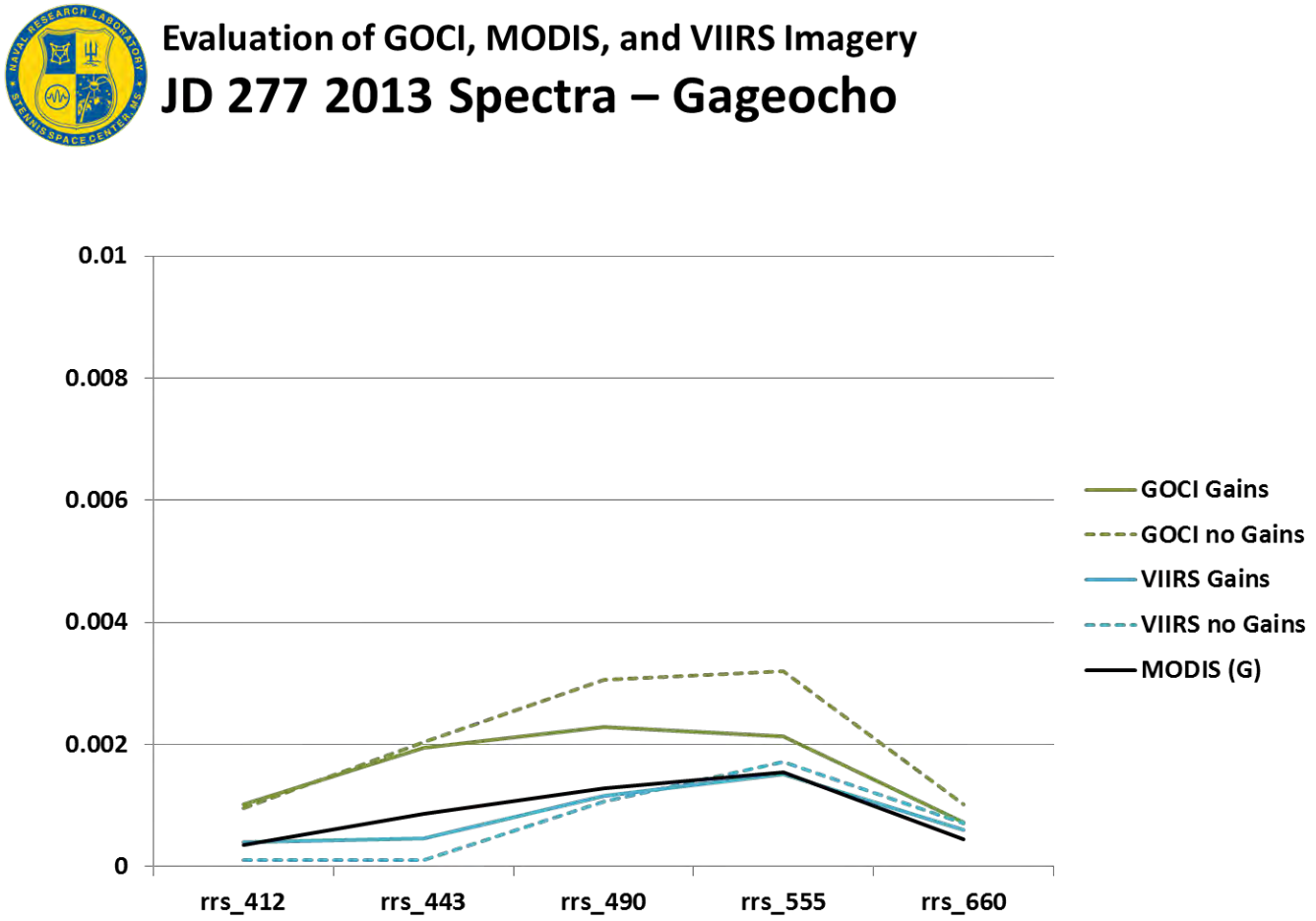

Figure 32 shows the spectral comparisons of the GOCI, VIIRS and MODIS sensors at the Gageocho station for Julian day 277, 2013. The MODIS data is processed with gains and shown as a black solid line. The VIIRS and GOCI data processed with gains are represented by solid lines. The VIIRS and GOCI data processed with unity gains (i.e., no gains) is denoted with dashed lines. *In situ* data was unavailable for this comparison. VIIRS and MODIS agree reasonably well with the exception of the 443 nm reflectance which is likely an effect of complex marine atmospheres typical in the coastal regions and the issues that arise with pixel to point comparisons. The GOCI data shows improvement with the gains applied however is higher than MODIS at all wavelengths.

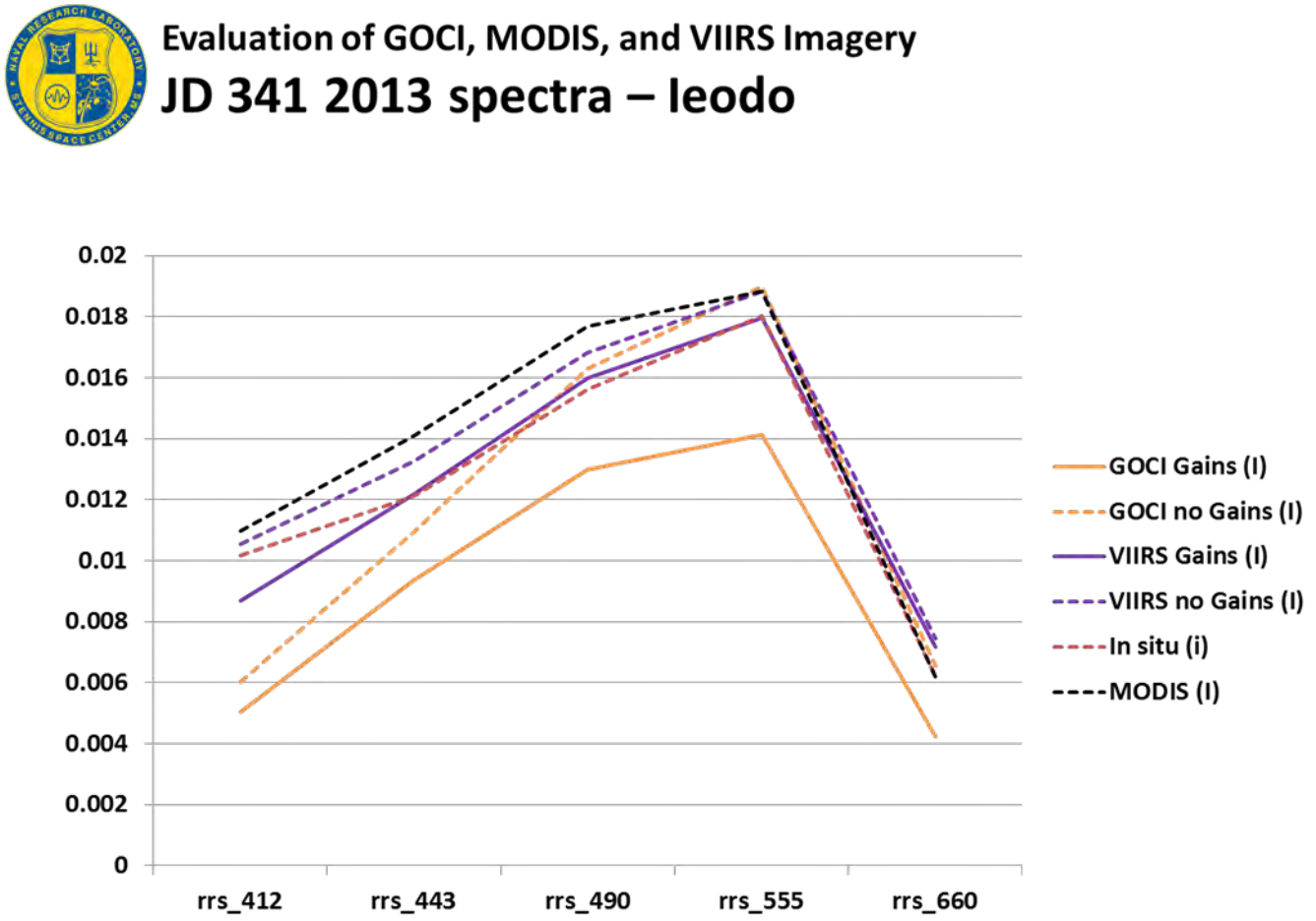

Figure 33 shows the spectral comparisons of the AOC, GOCI, VIIRS and MODIS sensors at the Ieodo station for Julian day 277, 2013. The *in situ* data at Ieodo is provided as the red dashed line. The MODIS data is processed with gains and shown as a black dashed line. The VIIRS and GOCI data processed with gains are represented by solid lines. The VIIRS and GOCI data processed with unity gains (i.e., no gains) is denoted with dashed lines. VIIRS and MODIS agree with regard to spectral shape however, with the gains applied the VIIRS shows lower reflectances at the lower wavelengths as compared to MODIS however VIIRS compares very well with the *in situ* data with a slight discrepancy at 412 nm. The GOCI data provides better retrievals in comparison to both MODIS an AOC without the gains applied. The GOCI without gains agrees better with AOC than MODIS for this date time combination.

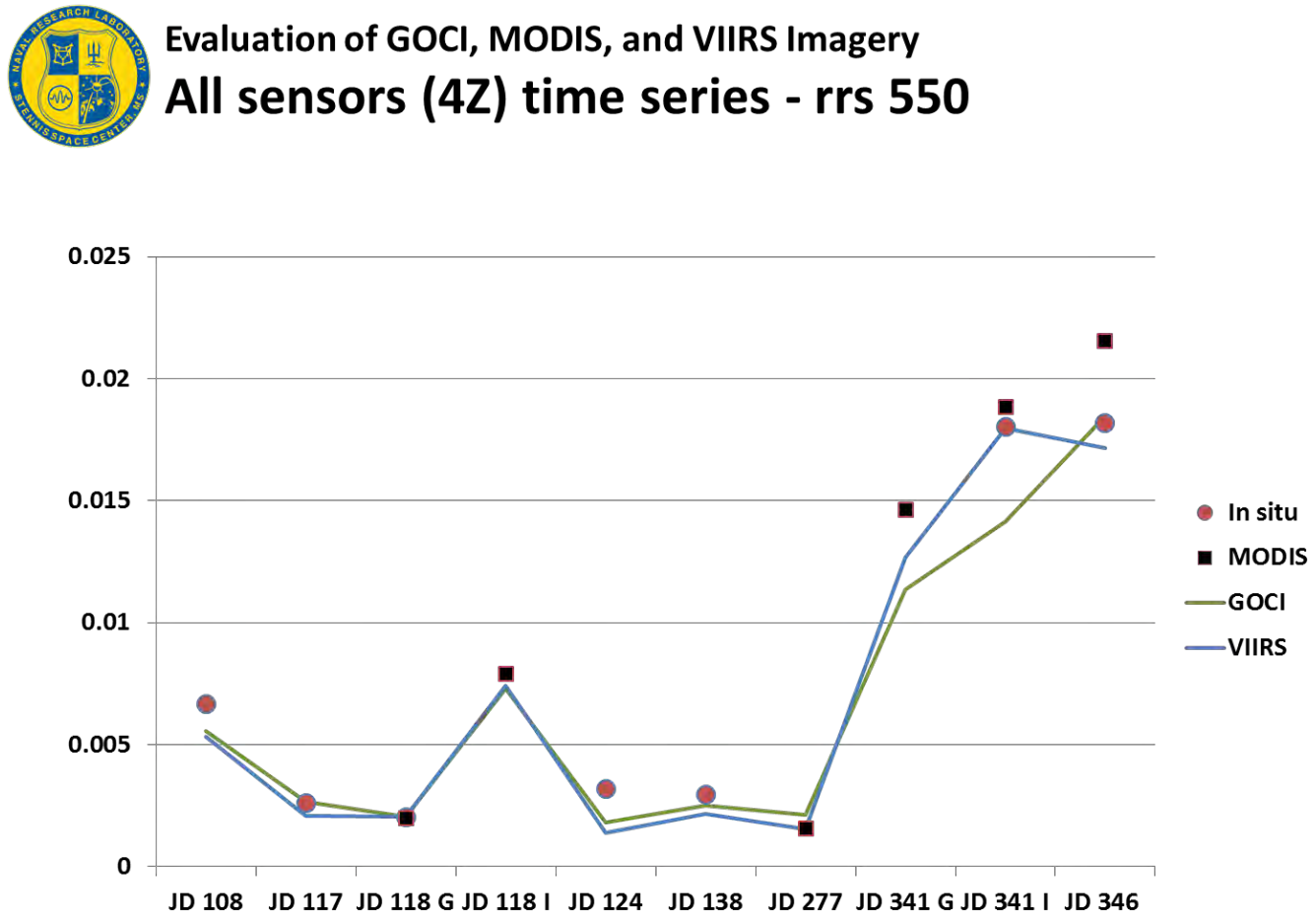

Figure 34 shows the time series of remote sensing reflectance at 550 nm for the *in situ* AOC, MODIS, GOCI, and VIIRS sensors. Data are shown for the 4 Zulu time to minimize sun glint and sensor issues.

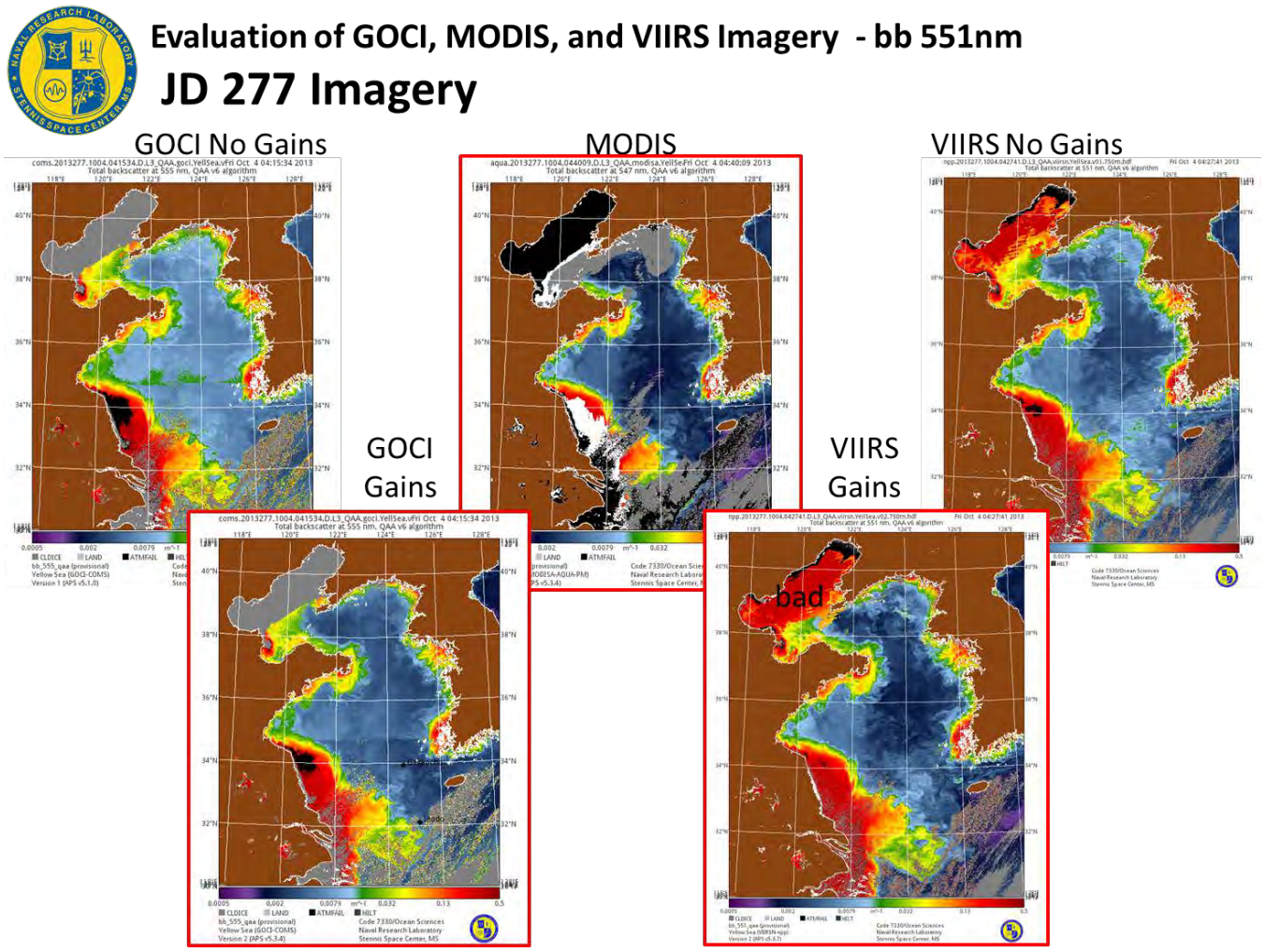

Figure 35 shows a visual comparison of GOCI, MODIS and VIIRS backscatter at 551 nm products for Julian day 277.

4 Operational Implementation

4.1 Operational Concept

The system will reside with NP3 at the Naval Oceanographic Office and automatically produce near real time (NRT) ocean color products from several satellites. Multiple real time satellite data streams of SDR (level 1) will be automatically processed, *via AOPS*, into Navy ocean optical products. Products produced by NAVOCEANO will support fleet operations and internal modeling efforts. Initial testing efforts have shown that approximately 1.25 hours are required to receive data from AFWA therefore an operational goal of approximately 2 hours to produce final products is reasonable.

Note: NAVOCEANO will not be pulling EDR's for Ocean Color as they intend to use the Navy algorithms to support operations.

4.2 Resource Requirements

The additional data storage requirements are being addressed within the NPOESS/ JPSS upgrades (A2).

4.3 Future Work

- Continue SAVANT updates and perform quarterly calibration and validation updates via the semi-automated "on-orbit vicarious calibration" technique. *This activity will also provide the ability to define the uncertainty of the inter-sensor products*
- Perform NRT Geostationary Ocean Color Imager (GOCI) initial cal/val to improve sensor performance by using Aeronet data (Ieodo) when available and synthetic Aeronet data from VIIRS selected at clear water sites
- Integrate frame correction for COMS GOCI to remove artifacts due to overlap and solar and sensor angles
- Perform a new cal/val for NPP VIIRS due to near-future updates to calibration coefficients / SDR's
- Implement band shift for desired wavelength (ex. 531nm) for IOP's using spectral models– LMI evaluation
- Improvements in sensor characterization, masking and algorithm development will be addressed as new versions of AOPS are transitioned to NAVOCEANO
- Improvements to the AOPS mosaicking capability
- Implement sharpening techniques to enhance VIIRS spatial resolution from 750m to 375m by using the VIIRS I-Bands
- Evaluate JPSS-1, Sentinel 3, GOCI-2 for operational products
- Establish data source for Sentinel-3A OLCI (ESA) w/proxy data for early/initial implementation (Underway with NOAA and NAVO)

5 Summary and Conclusions

The Navy's assessment of the Visible Infrared Imager Radiometer Suite (VIIRS) on Suomi National Polar-orbiting Partnership (NPP) indicates ocean color products are of high quality. Evaluations to date indicate the sensor meets Navy requirements for operational ocean optical products as demonstrated by comparison to both *in situ* data and as compared to current operational products derived from Moderate Resolution Imaging Spectroradiometer (MODIS). In both cases, VIIRS maintains a linear relationship with other accepted measurement techniques.

Spatial and temporal variability of bio-optical properties combined with differences in measurement techniques contribute to inconsistencies between remotely sensed and *in situ* measurements. We provide ground truth measurement for several ocean color sensors, VIIRS, MODIS, and GOCI at several sites around the world. Comparisons are shown for the various satellites and *in situ* measurements of nLw, rrs, a, bb and c using standard bio-optical algorithms. Discrepancies are attributed to imperfect

atmospheric corrections, uncertainties originating from sampling errors (including pixel to point matchups and including sea surface variations), and natural bio-optical variability.

Results indicate the VIIRS sensor will provide a continuous data stream to support operational navy products. VIIRS appears well characterized and is generating quality ocean color products as compared to existing ocean sensing satellites. The VIIRS sensor is capable of generating scientific research quality data in addition to meeting operational demands. Continued Cal/Val procedures are required to monitor ocean color product data stream for global trends and evaluate possible sensor degradation. As the JPSS Cal/Val Team (NASA, NOAA, and NRL) continues to better characterize the sensor and monitor the trends of the sensor's calibration tables, improvements to the generated ocean products are expected.

The NOAA operational SDR products from the IDPS are useable for navy products as has been demonstrated. However the present EDR ocean color products from NOAA's IDPS do not meet requirements to support Navy operations. Ocean color algorithms for the navy are unique. NOAA and NASA products do not meet navy requirements and are unlikely to do so in the foreseeable future. While the errors in coastal retrievals for nLw demonstrated in this report meet the accuracy goals and are lower than errors reported in literature (Chang, et al, Ladner et al), further improvements between satellite and *in situ* data can be made with improvements in the algorithms, although, that is beyond the scope of this work.

Based on initial validation results, we recommend proceeding with operational processing of VIIRS sensor data using the Navy's Automated Processing System, which is based on L2gen for ocean color products. Although continued monitoring and analyses will be required, the products should provide an adequate follow-on and replacement to MODIS to support Navy operations. The navy sees no reason that the VIIRS sensor should not provide scientific research quality data for new algorithm development and the capability to produce operational products to support the fleet as well as perform ecological monitoring in global ocean waters.

6 Technical References

Arnone, R.A, et al. 2012. *Monitoring Ocean Water Leaving Radiance for Inter-satellite Continuity*, Abstract ID: 12162, Ocean Sciences, Salt Lake City.

Bailey S.W. and P.J. Werdell, "A multi-sensor approach for the on-orbit validation of ocean color satellite data products", Rem. Sens. Environ. 102, 12-23 (2006).

Bailey, Sean W., Stanford B. Hooker, David Antoine, Bryan A. Franz, and P. Jeremy Werdell. 2008. *Sources and assumptions for the vicarious calibration of ocean color satellite observations,* Applied Optics, v 47, p2035.

Brown Steven W., Stephanie J. F., Feinholz M.E., Yarbrough M.A., Houlihan T., Peters D., Kim Y. S., Mueller J.L., Johnson B.C. and Clark D. K., "The Marine Optical BuoY (MOBY) radiometric calibration and uncertainty budget for ocean color satellite sensor vicarious calibration", SPIE Europe Remote Sensing, (2007).

Chang, C., Gould, R. 2006, Comparison of optical properties of the coastal ocean derived from satellite ocean color and in situ measurements, Optics Express v 14 No 22, 10149

Clark D., et al., "MOBY: A Radiometric Buoy for Performance Monitoring and Vicarious Calibration of Satellite Ocean Color Sensors: Measurements and Data Analyses Protocols" , Ocean Optics Protocols for Satellite Ocean Color Sensor Validation, Revision 4, Part VI, NASA Tech. Memo. 2003-210004/Rev 4./Vol. VI, NASA Goddard Space Flight, Greenbelt, Maryland, 3-34, (2003).

D'Alimonte, D., Zibordi, G. 2006. *Statistical assessment of radiometric measurements from autonomous systems,* IEEE Geosci. Remote Sens., v 44, p719.

D'Alimonte, D., Zibordi, G., Mélin, F.2008. A statistical method for generating cross-mission consistent normalized water leaving radiance, IEEE Trans. Geosci. Remote Sens., v46, p 4075.

Fargion G. S. et al. 2012. *Real time Cal/Val with Satellite Validation NAVY Tool (SAVANT)*, Abstract ID: 11090, Ocean Science Mtg, Salt Lake City.

Franz, Bryan A., Sean W. Bailey, P. Jeremy Werdell, and Charles R. McClain. 2007. *Sensor-independent approach to the vicarious calibration of satellite ocean color radiometry.* Applied Optics, v 46, p5068.

Hooker S.H., C McClain and A. Mannino, 2007: A Comprehensive Plan for the Long-Term Calibration and Validation of Oceanic Biogeochemical Satellite Data, NASA/SP-2007-214152, 1-40pp.

Ladner, S, Arnone, Gould and Martinolich, 2002. *Evaluation of SeaWiFS optical products in coastal regions*, Sea Technology v 43, p 29.

M. Wang, W. Shi, and L. Jiang, "Atmospheric correction using near-infrared bands for satellite ocean color data processing in the turbid western Pacific region," Opt. Express 20(2), 741–753 (2012).

Martinolich, Paul, 2012. *AOPS Users Guide v4.8*.

Mélin F, Zibordi G, Berthon J-F. 2007. *Assessment of satellite ocean color products at a coastal site*, Remote Sensing of Environment v 110, p 192.

Zibordi, Giuseppe, Brent Holben, Ily Slytsker, Davie Giules, Davide D' Alimonte, Fredreric Milin, Jean-Francois Berthon, Doug Vandemark, Hui Feng, Gregory Schuster, Bryan E. Fabbri, Seppt Kaitala, and Jukka Seppala. 2009. *AERONET-OC: A Network for the Validation of Ocean Color Primary Products*, Journal of Atmospheric and Oceanic Technology v 26, p1634.

7 List of Acronyms

Advanced Very High Resolution Radiometer (AVHRR)

Aerosol Optical Thickness (AOT)

Aerosol Robotic Network (AERONET)

Aerosol Robotic Network- Ocean Color (AERONET-OC)

Air Force Weather Agency (AFWA)

Anti-Submarine Warfare (ASW)

Automated Optical Processing System (AOPS)

Calibration and validation (Cal/val)

Colored dissolved organic matter (CDOM)

Comprehensive Large Array-data Stewardship System

Environmental Data Records (EDRs)

Expeditionary Warfare (EXW)

Geostationary Ocean Color Imager (GOCI)

Global Imager (GLI)

Government Resource for Algorithm Verification, Independent Testing and Evaluation (GRAVITE)

Graphical user interface (GUI)

Hierarchical Data Format (HDF)

Integrated Data Processing System (IDPS)

Japanese Ocean Color and Temperature Sensor (OCTS)

Joint Polar Orbiting System (JPSS)

Level 2 generator (L2Gen)

Look up table (LUT)

Marine Optical Buoy (MOBY)

Medium Resolution Imaging Spectrometer (MERIS)

Meteorology and Oceanography (METOC)

Mine Warfare (MIW)

Moderate Resolution Imaging Spectrometers (MODIS, on Terra and Aqua)

National Aeronautic and Space Administration (NASA)

National Center for Supercomputer Applications (NCSA)

National Oceanographic and Atmospheric Administration (NOAA)

National Polar-orbiting Observation Environmental Satellite System (NPOESS)

Naval Oceanographic Office (NAVOCEANO)

Naval Research Laboratory (NRL)

Naval Special Warfare (NSW)

Near infrared (NIR)

Near real time (NRT)

Normalized water leaving radiance (nLw)

Ocean Biology Processing Group (OBPG)

Ocean Colour Monitor (OCM)

Polarization Detection Environmental Radiometer (POLDER)

Quasi-Analytical Algorithm (QAA)

SAVANT - Satellite Validation Navy Tool

Sea-viewing Wide Field-of-view Sensor (SeaWiFS)

Space and Naval Warfare Systems Command (SPAWAR)

Suomi National Polar-orbiting Partnership (NPP)

Suspended particulate matter (SPM)

Total radiance signal at the top of the atmosphere (TOA)

Validation Test Report (VTR)

Visible Infrared Imager Radiometer Suite (VIIRS)